

# Engineering Principles for Scalable Connectomics

by

Monserrate Garzon Navarro

Submitted to the Department of Mechanical Engineering  
in partial fulfillment of the requirements for the degree of

BACHELOR OF SCIENCE IN MECHANICAL ENGINEERING

at the

MASSACHUSETTS INSTITUTE OF TECHNOLOGY

May 2025

© 2025 Monserrate Garzon Navarro. All rights reserved.

The author hereby grants to MIT a nonexclusive, worldwide, irrevocable, royalty-free license to exercise any and all rights under copyright, including to reproduce, preserve, distribute and publicly display copies of the thesis, or release the thesis under an open-access license.

Authored by: Monserrate Garzon Navarro  
Department of Mechanical Engineering  
May 9, 2025

Certified by: Martin L. Culpepper  
Professor of Mechanical Engineering, Thesis Supervisor

Accepted by: Daniel Frey  
Professor of Mechanical Engineering  
Undergraduate Officer, Department of Mechanical Engineering



# Engineering Principles for Scalable Connectomics

by

Monserrate Garzon Navarro

Submitted to the Department of Mechanical Engineering  
on May 9, 2025 in partial fulfillment of the requirements for the degree of

BACHELOR OF SCIENCE IN MECHANICAL ENGINEERING

## ABSTRACT

Brain tissue sectioning presents a significant challenge in connectomics, particularly when scaling to larger volumes. In the MICrONS 1 mm<sup>3</sup> mouse visual cortex dataset, 25.1% of scanned images—representing over a month of imaging work—were discarded due to sectioning defects. Current methods result in material loss during cutting and face limitations in tool wear and process efficiency. This thesis examines tissue sectioning through an engineering lens. Drawing from established machining practices and parallel industries, we propose and evaluate potential improvements to sectioning methods. The work aims to contribute to ongoing efforts in mapping larger connectomes, making it more practical and less error-prone.

Thesis supervisor: Martin L. Culpepper

Title: Professor of Mechanical Engineering



# Acknowledgments

I would like to thank Prof. Martin L. Culpepper for the opportunity to work on this project and for everything he taught me, both in class and through this thesis. Being part of his team was an incredible experience that pushed me to grow as an engineer. And of course, thank you to my family and friends for the support throughout this process and during my time at MIT.



# Contents

<i>List of Figures</i>	9
<i>List of Tables</i>	11
<b>1 Introduction</b>	<b>13</b>
1.1 Objectives and Scope	13
1.2 Background and Motivation	13
1.2.1 What is a Connectome?	13
1.2.2 Why Make Connectomes?	14
1.2.3 Major Accomplishments	15
1.2.4 The Future of Connectomics	19
1.3 Structure of the Thesis	20
<b>2 Theoretical Framework</b>	<b>21</b>
2.1 How to Make a Connectome	21
2.1.1 Specimen Preparation	21
2.1.2 Sectioning	22
2.1.3 Imaging	23
2.1.4 Reconstruction & Analysis	23
2.2 Material Properties of the Brain	24
2.3 Cutting Mechanics for Brain Tissue Sectioning	26
2.3.1 Fracture Modes	26
2.3.2 Stages of Cutting	27
2.3.3 Cutting Geometry	27
2.4 Energy-Based Modeling of Cutting Forces	28
<b>3 When Sectioning Fails</b>	<b>31</b>
3.1 Section Defects	32
3.1.1 Cracks & Folds	32
3.1.2 Partial Sections	35
3.1.3 Uneven Thickness	36
3.2 Material Losses from Sectioning	38
3.2.1 Inevitable Losses	39
3.2.2 Vibratomes	40
3.2.3 Knife Marks	41
3.3 Tool Wear and Maintenance	41

<b>4</b>	<b>Rethinking Sectioning</b>	<b>43</b>
4.1	Minimizing Forces to Improve Quality . . . . .	43
4.1.1	Slicing vs Chopping . . . . .	44
4.1.2	Embedding Mediums . . . . .	47
4.1.3	Lubrication to Lower Friction . . . . .	48
4.1.4	Assisted Cutting . . . . .	49
4.2	Improving Section Collection . . . . .	49
4.2.1	Direct Contact . . . . .	50
4.2.2	Vertical Collection System . . . . .	51
4.3	Introducing Automation . . . . .	52
4.3.1	Error Detection . . . . .	52
4.3.2	Dynamic Adjustment . . . . .	53
<b>5</b>	<b>Optimizing Connectomics for Scale</b>	<b>55</b>
5.1	Defining Success Metrics . . . . .	55
5.2	Optimization Model Breakdown . . . . .	56
5.3	Quantifying Sectioning Performance . . . . .	57
5.3.1	Quality . . . . .	57
5.3.2	Cumulative Factors: Cost and Time . . . . .	58
5.4	Sectioning Process Dependencies . . . . .	59
<b>6</b>	<b>Conclusion</b>	<b>61</b>
6.1	Key Contributions . . . . .	61
6.2	Future Work . . . . .	62
	<i>References</i>	63

# List of Figures

1.1	Connectomics Across Resolution Scales [4]	14
1.2	Complete Connectome of Hermaphrodite <i>Caenorhabditis elegans</i> [8]	16
1.3	Complete Connectome of 1st instar <i>D. melanogaster</i> larva [17]	16
1.4	Complete Connectome of 7-day-old adult female <i>D. melanogaster</i> [18]	17
1.5	Visual Cortex Subregions in the MICrONS Mouse Connectome (1 mm <sup>3</sup> ) [19]	17
1.6	Connectome of the Human Temporal Cortex (1 mm <sup>3</sup> ) [15]	18
1.7	Timeline and Scale of Major Connectomics Projects [20]	19
2.1	Specimen Preparation Workflow a) [21], b) [22], c) [23], d) [24]	22
2.2	Sectioning Workflow b) [25], d) [26], e) [27]	23
2.3	Modes of Fracture Analogy	26
2.4	Stages of Cutting Soft Tissue [32]	27
2.5	Microtome Geometry	28
3.1	Examples of Cracks and Folds in Sectioned Brain Tissue [36]	33
3.2	Failure Modes of the ATUM Collection System Leading to Tissue Section Damage	34
3.3	Blade Angle Changes Creating Complete versus Partial Sections	35
3.4	Correcting Blade-to-Block Misalignment [36]	36
3.5	Effect of Thermal Expansion on Ultramicrotome Section Thickness	37
3.6	Visualization of Compression in Sample Reconstruction	38
3.7	Soft Material Fracture Response Zone	39
3.8	Kerf Produced by the Vibratome	40
3.9	Built-Up Edge Formation on Cutting Tool During Metal Cutting [54]	41
4.1	Comparing Tomato Cutting Techniques [61]	44
4.2	Manual Brain Slicing Technique and Force Diagram [62]	45
4.3	Wire Slicer for Cutting Foam Sheets [64]	46
4.4	Horizontal Wood Veneer Slicer [65]	46
4.5	Industrial Cheese Slicer [66]	47
4.6	Different Loading Scenarios During Progressive Tissue Sectioning	48
4.7	Mode I Fracture on Sample Block	49
4.8	Travel Length of Section from Blade to ATUM [72]	50
4.9	Automated Tissue Section Capture System with Conveyor Transport [73]	51
4.10	Vertical Collection System for Ultrathin Sections	52

5.1	The Iron Triangle: Good, Fast, or Cheap [76] . . . . .	56
5.2	Overview of Optimization Model . . . . .	57
5.3	Map of Dependencies Relating Diamond Blade Wear . . . . .	59

# List of Tables

1.1	Comparative Analysis of Existing Connectomes . . . . .	15
2.1	Summary of Factors Influencing Brain Tissue Stiffness and Other Properties	25
3.1	Common Sectioning Errors and Their Associated Causes . . . . .	31
3.2	Sectioning and Imaging Losses in the 1 mm <sup>3</sup> Mouse Visual Cortex Dataset [16]	32
3.3	Section Usage in Mouse Visual Cortex and Fruit Fly Whole-Brain Connectomes	33
3.4	Thermal Expansion Estimates of Epoxy Resin During Sectioning . . . . .	37
3.5	Estimated Costs for Blade Switches for the 1 mm <sup>3</sup> Mouse and Human Connectomes . . . . .	42
4.1	Techniques for Mitigating Common Sectioning Errors . . . . .	43
5.1	Cost and Time Variables in the Sectioning Process . . . . .	58



# Chapter 1

## Introduction

### 1.1 Objectives and Scope

Sectioning brain tissue is one of the biggest bottlenecks in connectomics. Despite massive improvements in imaging and reconstruction, the tissue slicing and collection process remains fragile, inefficient, and poorly understood. This thesis takes an engineering approach to the problem, analyzing sectioning as a mechanical process shaped by cutting forces, material properties, and machine design. I break down how and why sections fail and draw on other industries to show how simple design changes could make the process more reliable. The result is a practical reference to improve sectioning outcomes and a foundation to scale connectomics beyond the limits of today.

Sectioning failures carry real costs. Cracks, folds, and uneven slices destroy valuable data before imaging even begins. These problems waste months of imaging time and severely limit the size and accuracy of connectomes. Tools such as microtomes and ATUM collectors have changed little in decades and offer no feedback or control over when or why failures occur. As imaging and reconstruction progress, sectioning has emerged as a limiting step, creating a clear need and opportunity to rethink and redesign how it is done.

Removing sectioning as a bottleneck will allow connectomics to scale with greater speed, reliability, and consistency. In turn, better connectomes will deepen our understanding of brain structure and function, supporting advances in neuroscience, medicine, and brain-inspired technology. This work offers a foundation for that future by showing that sectioning is not an inherent limitation, but rather a solvable engineering problem.

### 1.2 Background and Motivation

#### 1.2.1 What is a Connectome?

A connectome is a three-dimensional representation of the brain. Its purpose is to illustrate the intricate network of connections among neurons. This network is complex; for the human brain, it is estimated that the 86 million neurons each connect in thousands of ways, leading to trillions of connections [1].

We can study these complex networks at different scales of resolution, each revealing distinct aspects of brain connectivity. Not all connectomes are the same; the insights gained depend on the resolution of data acquisition. In the macroscale, connections between brain regions can be observed [2], while microscale analysis reveals individual neurons and the synapses linking them [3]. Figure 1.1 illustrates the resolution levels required for three different connectome scales.

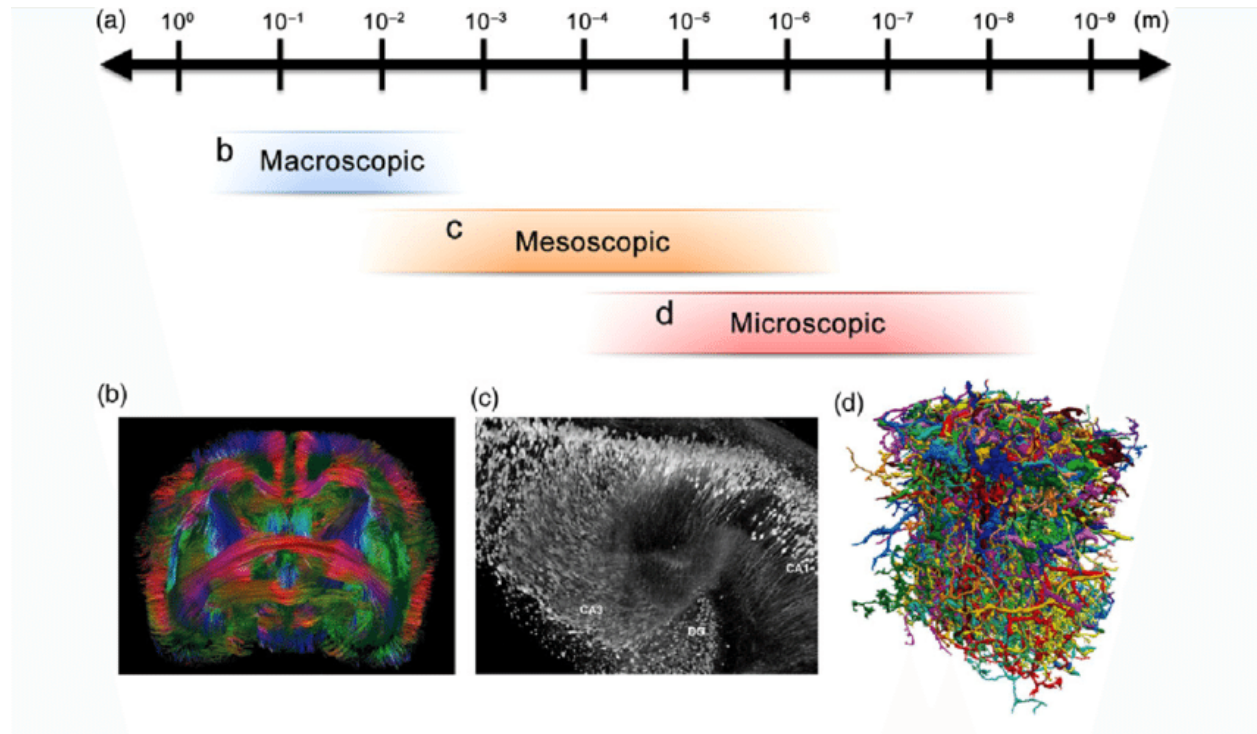


Figure 1.1: Connectomics Across Resolution Scales [4]

### 1.2.2 Why Make Connectomes?

Specialists in the field of connectomics believe that detailed maps of brains can reveal fundamental insight about brain function and therefore also about humankind. Sebastian Seung popularized this concept with the phrase “I am my connectome,” suggesting that the neural connections in our brain encode our individuality through holding not just the basic functions the brain needs but also memories and experiences [5]. Similar to how the human genome provides a blueprint of our genetic makeup, connectomes are believed to be the physical representation of our unique neural development shaped by both genetics and experiences.

Connectomes can create a window into understanding how the brain functions, from movement and sensation to learning and memory. By mapping how individual neurons communicate and identifying their types and roles, scientists can gain insights into the brain’s operational principles. Additionally, connectomes help us understand how neurological diseases develop by revealing structural abnormalities that may correspond to functional disruptions, potentially improving future detection and treatment methods.

### 1.2.3 Major Accomplishments

The foundations of connectomics were established as early as 1959, when E.G. Gray first applied electron microscopy to neural tissue [6]. This technical advancement enabled researchers to visualize the nervous system at a previously unattainable resolution. This was a critical step toward mapping the first connectome in 1986, that of the nematode *Caenorhabditis elegans*, with its simple total of 302 neurons [7].

Building on this foundational work, there have been major technological advances in electron microscopy and in reconstruction methods. Thanks to these advances, in 2019, researchers published complete, whole-animal connectomes for both sexes of *C. elegans*, offering extensive synaptic-resolution information of an entire animal nervous system [8]. This extended *C. elegans* connectome is shown in Figure 1.2.

Since these foundational achievements, connectomics has advanced in both scale and complexity. Table 1.1 summarizes key completed connectome projects, while Figures 1.2 through 1.6 illustrate these connectomes visually.

Table 1.1: Comparative Analysis of Existing Connectomes

Descriptor	<i>Drosophila melanogaster</i>	<i>Drosophila melanogaster</i>	<i>Platynereis dumerilii</i>	<i>Homo sapiens</i>	<i>Mus musculus</i>
Subject	1st instar larva	7-day-old	3-day Larva	45-year-old Female	Postnatal day 87 Male
Year	2023	2024 [9]	2025	2024	2025
Region	Whole Brain	Whole Brain [9]	Whole Body	Temporal Cortex	Visual Cortex
Volume (mm <sup>3</sup> )	—	0.08	$4.68 \times 10^{-3*}$	1.05	0.93
Sectioning Method	Leica UC6 [10]	Leica UC6	RJ Ultracut E [11]	ATUM	ATUM
Collection Method	Manual [10]	Manual	Manual	ATUM	ATUM
Imaging Method	TEM [10]	TEM	TEM	mSEM	TEM
Section Count	4,841	7,062	4,846	5,019	19,974**
Thickness (nm)	50 [10]	35-40	40	33.9 †	40
Neuron Count	3,016	139,255 [9]	966	16,087	84,035

\* Calculated value

† Average section thickness

Default references (unless otherwise specified): [12] for first *D. melanogaster*, [13] for second *D. melanogaster*, [14] for *P. dumerilii*, [15] for *H. sapiens*, [16] for *M. musculus*.

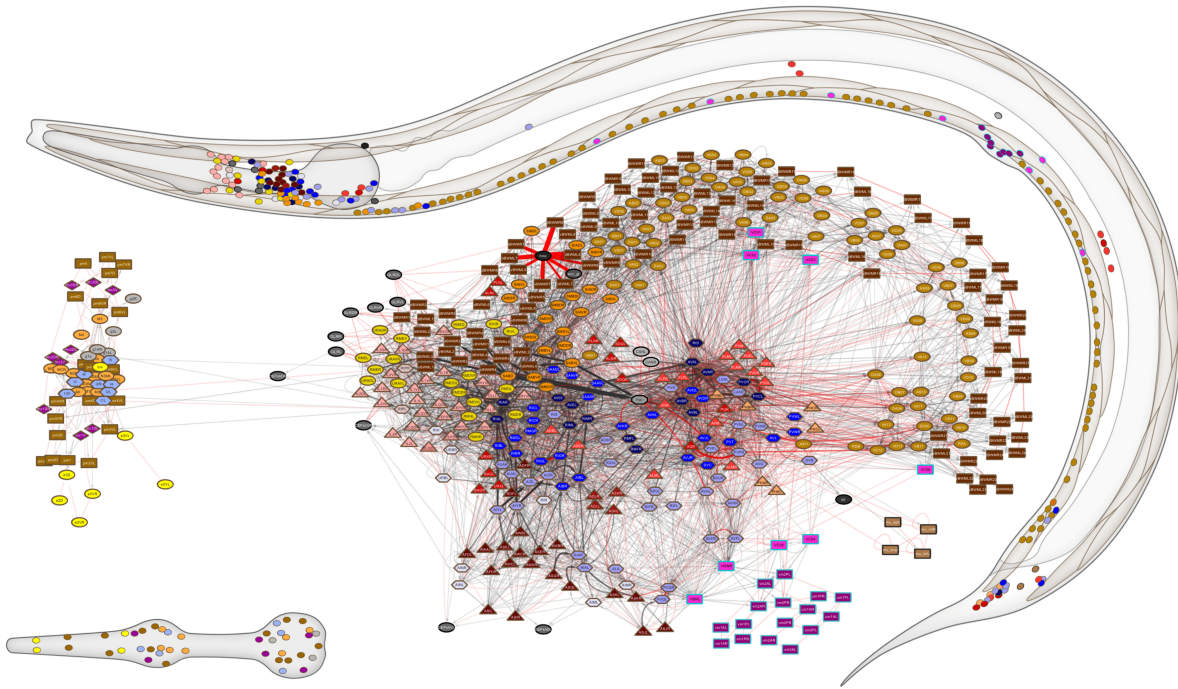


Figure 1.2: Complete Connectome of Hermaphrodite *Caenorhabditis elegans* [8]

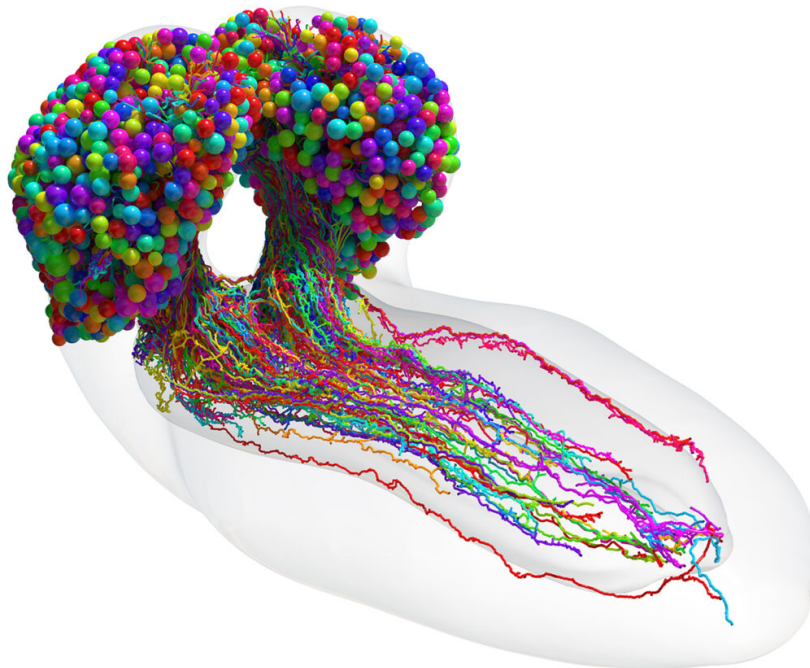


Figure 1.3: Complete Connectome of 1st instar *D. melanogaster* larva [17]



Figure 1.4: Complete Connectome of 7-day-old adult female *D. melanogaster* [18]

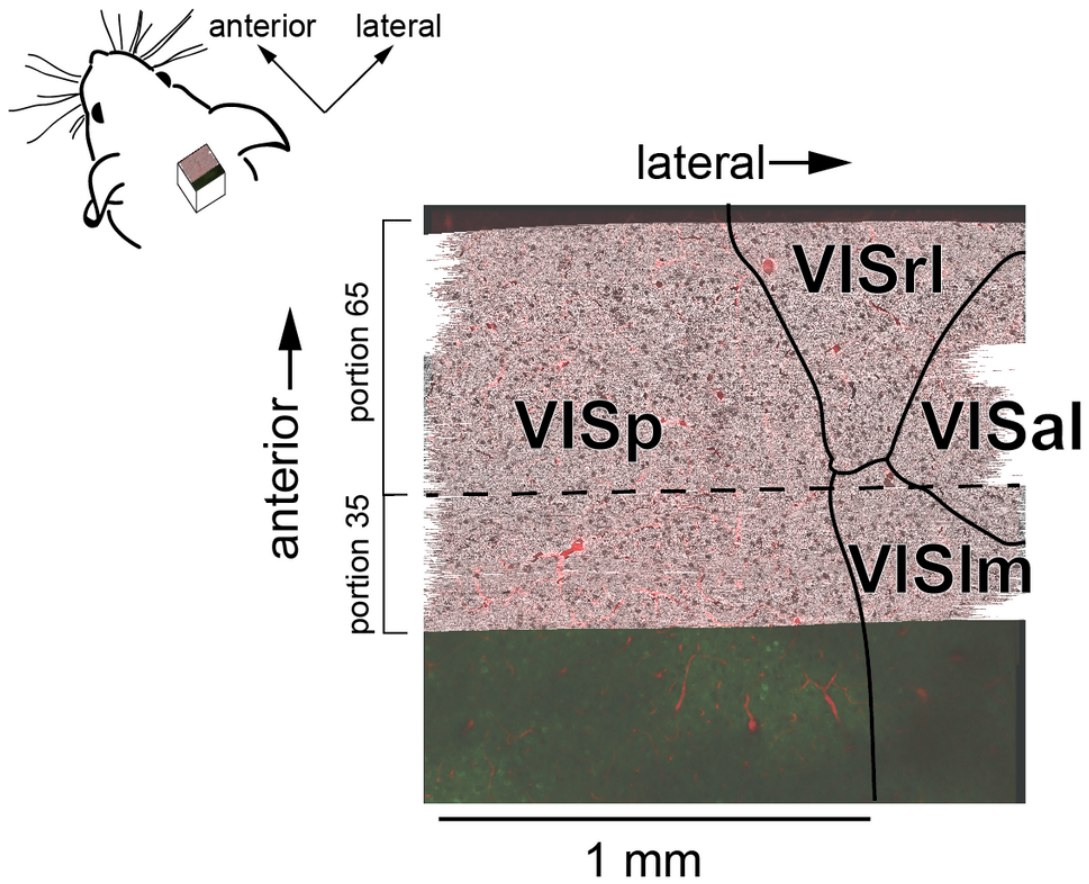


Figure 1.5: Visual Cortex Subregions in the MICrONS Mouse Connectome ( $1 \text{ mm}^3$ ) [19]

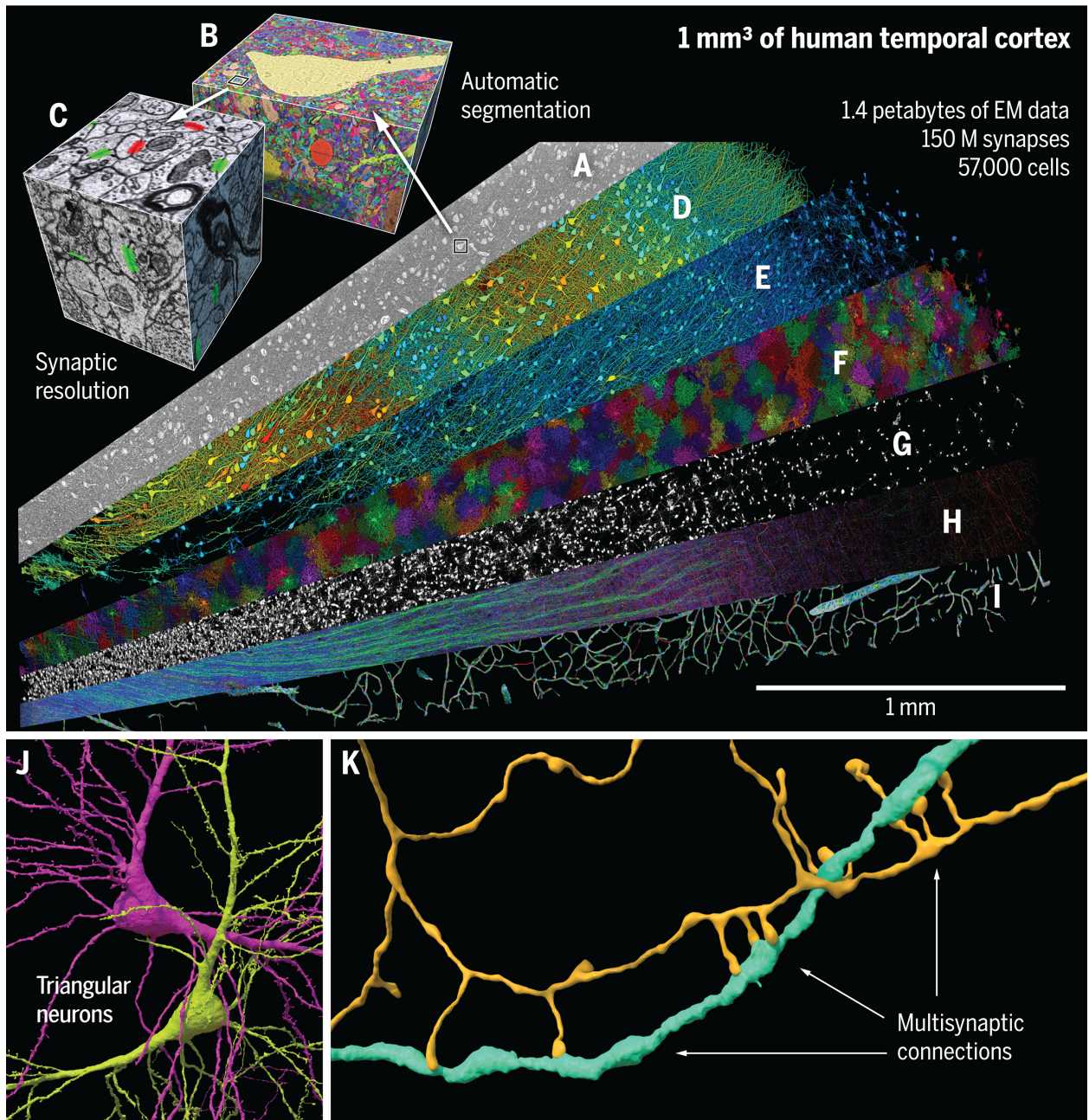


Figure 1.6: Connectome of the Human Temporal Cortex (1 mm<sup>3</sup>) [15]

## 1.2.4 The Future of Connectomics

The ultimate goal in connectomics is to map mammalian brains in their entirety. The mouse hippocampus connectome is the following intermediate milestone. Google, along with other research teams, has recognized this structure as a crucial aim that strikes a balance between technical viability and scientific significance [20]. The mouse hippocampus alone is orders of magnitude more complicated than completed connectomes, as shown in Figure 1.7, both in terms of the amount of storage and number of neurons.

### Landmark Connectomics Projects







Project		Complexity	Storage	Timeline
<i>C. elegans</i> roundworm		302 neurons	Terabytes	1970s-1986
<i>Drosophila</i> fruit fly		125,000 neurons	Tens of terabytes	2010-2023
Human brain (fragment)		16,087 neurons	1.4 petabytes	2018-2021
<b>Mouse hippocampus</b>		<b>1,000,000 neurons</b>	<b>25 petabytes</b>	<b>2023-2028</b>
Mouse		100,000,000 neurons	Hundreds of petabytes	2023-?
Human brain (whole)		100,000,000,000 neurons	Hundreds of exabytes	?

Figure 1.7: Timeline and Scale of Major Connectomics Projects [20]

Researchers must rethink current methods to overcome the core bottlenecks that limit the scalability and accuracy of connectome reconstruction. Notably, recent large-scale projects have encountered significant problems with data quality, primarily stemming from automated collection techniques. While these automation methods offer the higher throughput necessary for mapping larger volumes, they substantially compromise tissue integrity and image quality, resulting in wasted imaging time on unusable sections and necessitating more complex data processing to compensate for artifacts and errors. This quality-throughput trade-off will be an issue as the projects scale up, creating a fundamental challenge for advancing the field.

## 1.3 Structure of the Thesis

The structure of the thesis is as follows:

- **Chapter 2** provides the background needed to understand the ideas developed throughout the thesis.
- **Chapter 3** explores key issues in the sectioning process that are creating a central bottleneck in scaling connectomics.
- **Chapter 4** proposes solutions to improve the quality of the sections produced.
- **Chapter 5** pivots the focus to a broader systems-level view, by proposing modeling and optimization techniques to help efficiently scale connectomics.
- **Chapter 6** concludes by discussing the work's broader implications for engineering and large-scale connectomics.

# Chapter 2

## Theoretical Framework

This chapter provides a technical foundation for understanding later discussions on issues with the current process and potential solutions.

### 2.1 How to Make a Connectome

The connectomics process can be broken down into four main steps:

1. **Specimen Preparation:** This can include in vivo experiments, followed by brain harvesting, fixation, dehydration, labeling, and embedding for sectioning.
2. **Sectioning:** Involves cutting the brain into ultrathin slices, which together form the individual layers that make up the complete connectome.
3. **Imaging:** The examination of the sample with a high-resolution microscope to capture the neural structures and synapses of the sample.
4. **Reconstruction & Analysis:** The development of the digital model using manual or automated techniques.

#### 2.1.1 Specimen Preparation

Maintaining the structure of the brain on the nanoscale is essential for connectomics. The goal is to minimize structural deterioration between living and harvested tissue. Effective stabilization of brain tissue ensures that synapses, organelles, and cellular boundaries remain intact throughout the sectioning and imaging processes.

Although protocols can vary according to the organism or specific research goals, the following steps are generally carried out to prepare the sample, as illustrated in Figure 2.1:

1. **In-Vivo Experiments:** During this phase, neural activity data is collected in response to various stimuli in the living specimen. These measurements form the basis for the ‘functional connectome’ that researchers use to gain insight into brain function and establish a relationship to the structural connectome produced in subsequent steps.

2. **Harvesting:** Removal of the brain or region of interest. During this process, certain ethical guidelines must be followed.
3. **Fixation:** Stabilizes the tissue structure. Occurs either before or after (perfusion vs. immersion) harvesting, depending on the organism size.
4. **Labeling:** Enhances contrast in imaging. Markers (e.g. antibodies or chemical stains) bind to specific structures or components of the brain, making them more visible under the chosen imaging method.
5. **Dehydration:** Removal of water from tissue to help with the infiltration of the embedding medium.
6. **Embedding:** This step wraps the tissue in a solid medium. The medium provides structural support during the sectioning of ultrathin slices.

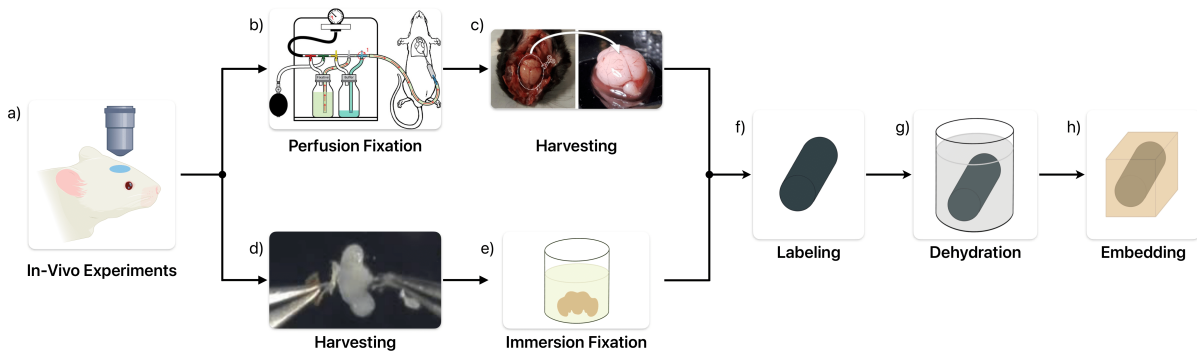


Figure 2.1: Specimen Preparation Workflow a) [21], b) [22], c) [23], d) [24]

### 2.1.2 Sectioning

To properly visualize synapses, brain tissue must be sliced into ultrathin sections. Creating smooth, defect-free cuts and successfully collecting each section is challenging due to their extreme fragility and near-invisibility to the naked eye. This step fundamentally determines the maximum quality and resolution achievable in the final connectome.

The following steps typically occur in the sectioning workflow, as shown in Figure 2.2:

1. **Trimming:** Removal of excess embedding medium surrounding the sample, improving sectioning efficiency, and potentially reducing imaging time in systems that lack automatic detection of empty resin areas.
2. **Sample-Blade Alignment:** Repositioning of the sample to be at the correct angle with the edge of the blade for effective sectioning.
3. **Sectioning:** Ultrathin sections (30-50 nm) are cut with a microtome and a diamond knife.

4. **Collection:** The water bath captures each newly cut section as it falls from the microtome. Operators either manually transfer the section to an imaging grid or use the ATUM (Automated Tape-collecting Ultra-Microtome) system, with a conveyor belt that automatically collects sections.

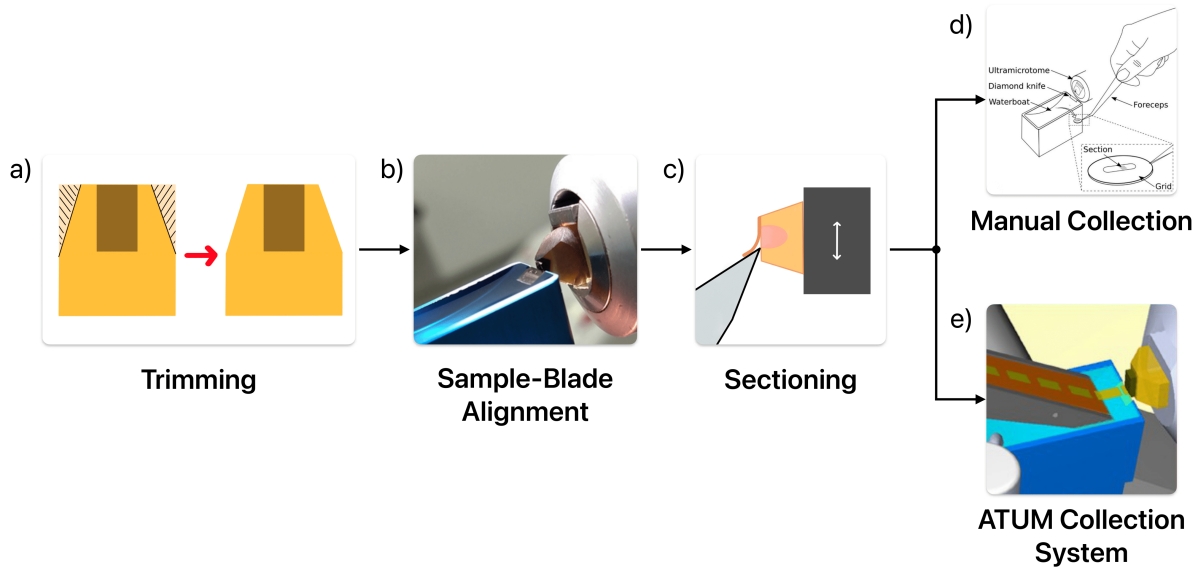


Figure 2.2: Sectioning Workflow b) [25], d) [26], e) [27]

### 2.1.3 Imaging

After sectioning, transmission electron microscopy (TEM) is typically used to image the tissue. Alternative methods include multibeam scanning electron microscopy (mSEM) and serial block-face SEM (SBF-SEM), which are designed to image larger tissue volumes. Due to the specific complexities associated with each microscopy system, this thesis does not discuss them in detail.

### 2.1.4 Reconstruction & Analysis

The brain images are assembled into a 3D volume by stacking each layer. Errors such as missing tiles, missing sections, or lost sections should be accounted for either manually or with automatic tools. Once assembled, segmentation identifies neurons, synapses, and cellular structures either manually or with machine learning. Finally, proofreading ensures accuracy by reviewing and correcting errors in automated segmentation.

## 2.2 Material Properties of the Brain

Brain tissue exhibits complex mechanical behavior, distinguishing it from rigid materials like metals or ceramics. Several factors, such as the applied forces, water content, species, age, and pathological conditions influence this behavior [28]. All these variables make testing and modeling brain tissue particularly challenging.

The mechanical properties of brain tissue, specifically its stiffness, are critical across many stages of the connectome pipeline. During sectioning, tissue stiffness determines the cutting forces, directly impacting tool wear and blade longevity. In post-cutting stages, these properties influence how sections behave during collection and mounting. Stiffer tissue can resist deformation but may be prone to cracking, while softer tissue might stretch more. Understanding and quantifying these mechanical properties enables immediate process improvements that can optimize tool geometry, adjust cutting speeds to reduce wear, and minimize tissue deformation. This understanding remains crucial as it informs how we can safely manipulate and process brain tissue in any new approaches we develop.

Unfortunately, there is no single simple value to describe the stiffness of the brain, and current research does not provide direct insights because the testing conditions do not necessarily match what occurs during the connectomics process. However, several key factors are known to influence stiffness. Table 2.1 draws extensively from the comprehensive review by Budday et al. [28], which compiled findings from multiple experimental studies.

Category	Factors
<b>Increases Brain Tissue Stiffness</b>	<ul style="list-style-type: none"> <li>• Higher myelin content</li> <li>• Increased strain and strain rate</li> <li>• Development (due to increased myelination)</li> <li>• In vivo conditions (compared to ex vivo)</li> <li>• Loading phase (compared to unloading, due to hysteresis)</li> </ul>
<b>Decreases Brain Tissue Stiffness</b>	<ul style="list-style-type: none"> <li>• Higher water content (gray matter at 0.83 g/ml vs. white matter at 0.71 g/ml)</li> <li>• Higher temperatures</li> <li>• Ex vivo conditions (due to hydration and biochemical changes)</li> <li>• Preconditioning through repeated loading (temporary effect)</li> <li>• Pathological conditions (e.g., multiple sclerosis, Alzheimer’s disease, demyelination)</li> </ul>
<b>Other Notable Properties</b>	<ul style="list-style-type: none"> <li>• White and gray matter exhibit distinct mechanical responses</li> <li>• Generally isotropic despite structural variations</li> <li>• Hysteretic behavior (different response during loading vs. unloading)</li> </ul>

Table 2.1: Summary of Factors Influencing Brain Tissue Stiffness and Other Properties

In other machining processes, mechanical characterization has historically been essential for managing advanced materials and improving manufacturing efficiency [29]. More research should be done in this area to fully understand the practical implications of these properties and their effects on connectome creation. This is particularly important when modeling tissue sectioning, handling, and tool wear, factors that must be optimized to achieve our primary objectives, such as producing high-quality sections.

## 2.3 Cutting Mechanics for Brain Tissue Sectioning

Building on the mechanical properties of brain tissue, understanding fracture mechanics is critical for optimizing cutting tools and techniques in connectomics. Proper sectioning minimizes tissue deformation, preserves structural integrity, and improves tool longevity. Fracture theory provides a framework to describe how cutting forces interact with materials, which is especially relevant for brain tissue's unique properties.

### 2.3.1 Fracture Modes

A key thing to know about fracture theory is that there are three main ways to initiate and propagate a crack [30]. These modes describe the relative motion of crack surfaces during failure. Figure 2.3 illustrates the motions of each mode.

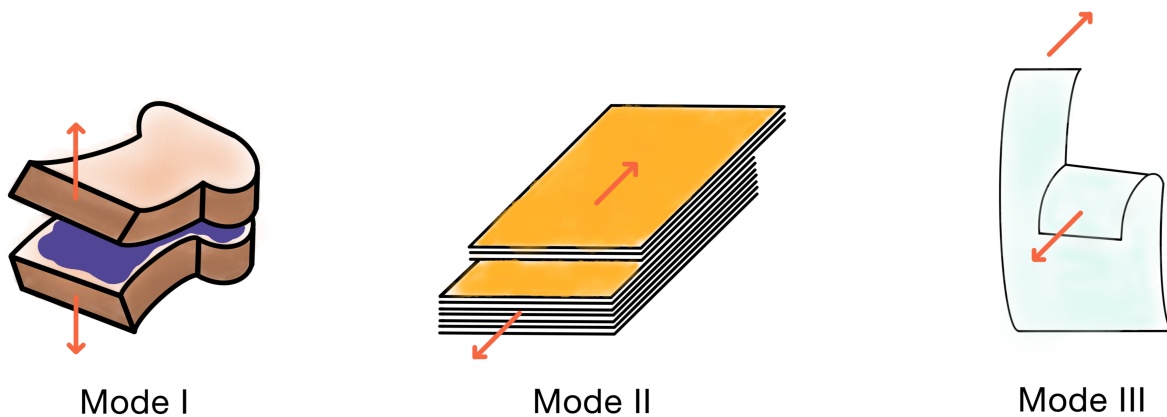


Figure 2.3: Modes of Fracture Analogy

- **Mode I** This is like pulling apart a sandwich. Imagine gripping the top and bottom and pulling them straight apart. The crack opens vertically, with the surfaces moving directly away from each other.
- **Mode II** Picture pushing a deck of cards so the top slides forward and the bottom slides backward. The crack surfaces move horizontally past each other, like sliding doors moving in opposite directions.
- **Mode III** This is like tearing a piece of paper by twisting your hands in opposite directions. The surfaces move sideways relative to each other as the crack opens.

A microtome operates primarily in Mode I; the blade functions as a wedge that pulls apart sections. A vibratome, on the other hand, combines Mode I and Mode II, creating both opening and shearing forces. These cutting mechanics and their implications are explored further in Chapters 3 and 4.

### 2.3.2 Stages of Cutting

Research on soft tissue cutting has been driven primarily by surgical applications, particularly to develop automated surgical robots. Through this work, researchers have established that the cutting process follows three distinct stages [31, 32]:

1. **Deformation Stage:** When the blade first touches the tissue, it pushes and squishes the tissue without actually cutting through it. During this time, energy builds up in the compressed tissue.
2. **Rupture State:** Once enough force is applied, the built-up energy is suddenly released as the tissue begins to break apart, and the cutting force drops sharply.
3. **Cutting Stage:** The cutting process starts off uneven but eventually settles into a smooth, continuous cutting motion with steady forces as the blade moves through the tissue.

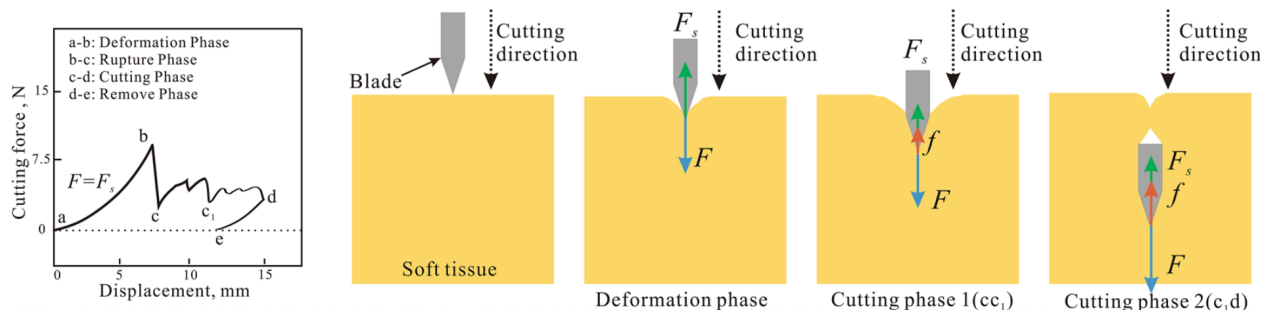


Figure 2.4: Stages of Cutting Soft Tissue [32]

Figure 2.4 depicts the cutting process, with the force-displacement curve (left) showing the forces involved during each stage, and the illustrations (right) demonstrating the physical progression of blade-tissue interaction through each phase. This highlights the importance of separating each stage, as the cutting force can vary dramatically, decreasing by nearly 80% during the rupture phase alone before stabilizing at lower forces during steady-state cutting. Brain tissue sectioning likely follows a similar pattern, and quantifying this could enable the optimization of cutting parameters, such as blade speed and angle, to minimize tissue deformation, improve section quality, and ensure consistency.

### 2.3.3 Cutting Geometry

This section provides a basic representation of the microtome blade and the geometry of the brain sections, highlighting the key parameters that influence the cutting process. Figure 2.5 shows the relevant variables, including the blade angle ( $\theta$ ), clearance angle ( $\alpha$ ), section curvature ( $R$ ), tip radius ( $r$ ), cutting speed ( $v$ ) and the thickness of the section ( $t$ ).

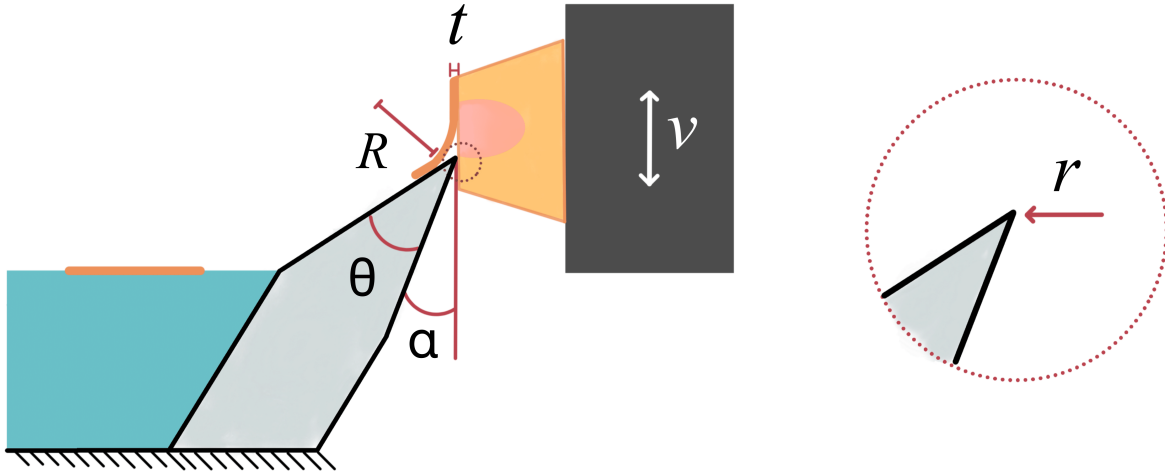


Figure 2.5: Microtome Geometry

Optimizing these parameters is essential for reducing friction, preventing tissue curling, and maintaining structural integrity during sectioning. These aspects are critical for achieving consistent, high-quality slices for connectomics analysis.

## 2.4 Energy-Based Modeling of Cutting Forces

Modeling cutting forces helps define the sectioning process and provides a foundation for more consistent results and more accurate connectomes. To avoid damage, cutting should be as efficient as possible, as any excess force beyond what is needed to fracture the tissue is absorbed through deformation. Fine-tuning cutting parameters and enabling real-time control can help maintain this efficiency and reduce sectioning errors.

Although there are well-developed models for metal cutting, supported by extensive empirical data [29], comparable models for brain tissue sectioning are largely unavailable. However, an energy conservation model provides a simple starting point to estimate cutting forces [31, 33, 34]. This approach estimates the minimum energy required for cutting while accounting for various inefficiencies, such as tissue deformation.

Material property characterization of brain tissue has direct relevance to traumatic brain injury research, particularly the measurement of fracture energy [35]. Although these measurements were conducted under different conditions than those used in connectomics, they provide a valuable baseline estimate. Fracture energy, measured in  $\text{J}/\text{m}^2$ , quantifies the energy required to create a crack with a characteristic area determined by the depth and width of the newly formed surface. This metric is commonly used in energy conservation models like the one described below.

The total energy applied by the tool ( $E_{\text{tool}}$ ) during cutting can be expressed as:

$$E_{\text{tool}} = E_{\text{fracture}} + E_{\text{elastic}} + E_{\text{plastic}} + E_{\text{friction}} + E_{\text{losses}}$$

where:

- $E_{\text{fracture}}$ : Energy required to create a crack in the tissue.
- $E_{\text{elastic}}$ : Energy temporarily stored as elastic deformation within the tissue.
- $E_{\text{plastic}}$ : Energy dissipated due to irreversible plastic deformation of the tissue.
- $E_{\text{friction}}$ : Energy lost due to friction at the interface between the blade and the tissue.
- $E_{\text{losses}}$ : Miscellaneous energy losses, such as heat generation or viscous damping effects.

The energy required to create a crack ( $E_{\text{fracture}}$ ) depends on the fracture toughness ( $G_c$ ) of the tissue and the area of the newly formed crack ( $A$ ). It can be expressed as:

$$E_{\text{fracture}} = G_c \cdot A$$

where:

- $G_c$ : Fracture toughness, representing the energy per unit area required to initiate a crack.
- $A$ : Area of the cutting path, determined by the blade width and depth of cut ( $A = \text{Blade Width} \times \text{Depth of Cut}$ ).

This energy-based model breaks down the main energy sources in the cutting process such as fracture, friction, and deformation. By identifying where excess energy is consumed beyond what is needed for fracture, we can target design improvements that minimize inefficiencies and reduce tissue section damage. Future work will involve empirically validating and determining physical properties, such as fracture toughness, then developing more complex force models correlated to process parameters such as blade geometry, embedding media, and cutting speed.



# Chapter 3

## When Sectioning Fails

Among the many challenges in scaling connectomics, the sectioning process stands out as a critical limitation and serves as the focus of this chapter. The issues at the heart of this process boil down to two key factors: (1) the microtome has remained fundamentally unchanged since the first connectome was produced in 1986, and (2) current attempts at automating section collection contribute to section damage and reduced quality prior to imaging.

The two largest synapse-level connectomes to date, each spanning 1 mm<sup>3</sup> of mouse visual cortex and human temporal cortex, highlight how sectioning issues become more prevalent at larger scales. The level of physical damage in these datasets is noticeably higher than in smaller connectomes, largely due to the lack of innovation in microtome design and the introduction of the ATUM system as a replacement for manual collection.

Although advanced reconstruction techniques can help mitigate these issues, they cannot precisely recreate the lost information. These errors not only compromise the quality of the connectome, but also result in many cut and imaged sections becoming unusable, wasting valuable resources and equipment.

This chapter examines the root causes of sectioning failures to convert seemingly unpredictable problems into solvable challenges. Table 3.1 summarizes the key failures in the sectioning process, each discussed further in the subchapters that follow.

Cause	Cracks	Folds	Uneven Thickness	Partial Sections	Material Loss	Knife Wear
Microtome	✓	✓	✓	✓	✓	✓
ATUM*	✓	✓				

\* These errors existed previously, but have become more frequent with ATUM use.

Table 3.1: Common Sectioning Errors and Their Associated Causes

## 3.1 Section Defects

This subchapter analyzes surface-level errors that occur during the cutting process and affect image quality. Three primary defects are particularly relevant: (1) cracks and folds, (2) partial sections, and (3) uneven thickness. These defects compromise section quality before the imaging stage even begins.

Unfortunately, these errors are difficult to detect prior to imaging, meaning that defects often only become apparent once a section has been cut and imaged. In some cases, it is worth proceeding with the scanning just to definitively determine whether a questionable section is usable for the final dataset. Depending on severity, affected images may be excluded from the final connectome, wasting both the sectioning and imaging resources invested in producing that layer.

Table 3.2 illustrates this problem using the MICrONs 1 mm<sup>3</sup> mouse visual cortex dataset. Most strikingly, approximately 25.1% of scanned data, representing nearly two months of imaging work, was ultimately excluded due to severe sectioning defects [16]. Even among the accepted sections, numerous errors complicated the reconstruction process, creating additional challenges for connectome assembly [36].

<b>Sectioning</b>	<b>Value</b>
Total Time	12 days
Wasted Time	3.4 days
Sections Discarded	28.6%
<b>Imaging</b>	<b>Value</b>
Total Time	6 months
Wasted Time	1.5 months
Images Discarded	25.1%

Table 3.2: Sectioning and Imaging Losses in the 1 mm<sup>3</sup> Mouse Visual Cortex Dataset [16]

Although errors like these are disclosed in the articles, the underlying causes are not addressed, leaving room for speculation. Here, we define the defects and the potential factors that cause them. Despite its long history, connectomics research continues to rely heavily on traditional microtome methods for brain tissue sectioning. This dependence on conventional techniques suggests significant potential for methodological innovation. To properly scale the field, sectioning techniques must undergo a fundamental change.

### 3.1.1 Cracks & Folds

Cracks and folds are two major defects that create discontinuities in tissue section images, distorting the accuracy of the images of the collected sections. Cracks (Figure 3.1c) form when tensile forces pull the section apart at weak points, resulting in two destructive effects: the creation of physical gaps and irreversible damage to tissue features along the edges of the crack. Folds (Figure 3.1a) occur when the section buckles, causing the previously flat surface to adhere to itself and obscure all the information within the folded region. In severe cases,

both types of damage can result in complete loss of critical neural structures, including entire cell bodies [36].

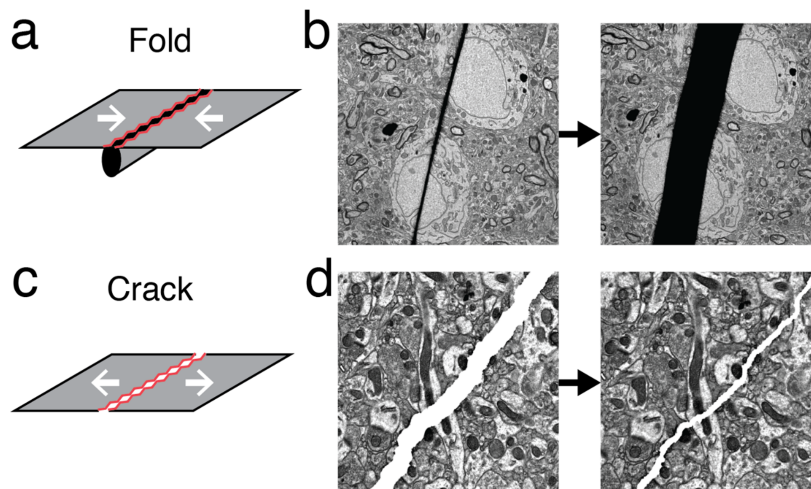


Figure 3.1: Examples of Cracks and Folds in Sectioned Brain Tissue [36]

During the reconstruction of the MICrONS 1 mm<sup>3</sup> mouse dataset, researchers found that “virtually every section had developed numerous cracks and folds” [36]. These defects were present even in the final connectome images, after the unusable images had already been removed from the dataset. Although the MICrONS project had previously developed realignment tools during their pilot-scale version, these tools proved inadequate for the 1 mm<sup>3</sup> dataset. This was because the larger dataset contained far more extensive and complex image defects than in the pilot study, rather than just a proportional increase in the same types of defects.

### Potential Causes

Collection methods differed significantly between projects. Despite the seemingly more efficient ATUM system, the larger study saw more sectioning defects than the pilot study, which relied on manual methods [16, 36]. Compared to the fruit fly full brain connectome project, the error rates do not scale proportionally. Table 3.3 illustrates the substantial difference in efficiency: 96.8% of sections were successfully utilized for the fruit fly project versus only 71.4% for the mouse project. A key distinguishing factor appears to be the collection method, as the fruit fly sections were collected manually rather than through automated systems.

Metric	Mouse – 1mm <sup>3</sup> Visual Cortex [16]	Fruit Fly – Full Brain [13]
Collection Method	ATUM	Manual
Total Sections	27,972	7,062
Sections Imaged	26,652 (95.3%)	7,050 (99.8%)
Sections in Connectome	19,974 (71.4%)	6,839 (96.8%)

Table 3.3: Section Usage in Mouse Visual Cortex and Fruit Fly Whole-Brain Connectomes

The ATUM system uses a TEM compatible film ‘tape’ to collect and preserve the sample for subsequent scanning [37]. A key feature of this tape is its ‘wettability’, which allows samples to adhere to its surface [38]. Although this strong adhesion is beneficial for sample retention, it can create cracks and folds. Below are a couple of scenarios during the collection process that are likely to contribute to the defects:

1. **Opposing forces during transfer:** The stickiness of the tape and the drag from the water create forces that act in opposite directions, putting the tissue section under tension, as shown in Figure 3.2b. This tension can exceed the yield strength of the section, resulting in crack formation.
2. **Bending stress during transfer:** The angle at which the ATUM collects sections from the water causes the section to bend. This creates a stress gradient where the lower surface is in tension while the upper surface is in compression, as shown in Figure 3.2c. If high enough, this stress might cause the section to crack.
3. **Velocity mismatch:** When the section approaches the ATUM at a speed greater than the ATUM collection speed, the section may curl onto itself before the tape advances sufficiently to allow the section to adhere flatly, as illustrated in Figure 3.2d.

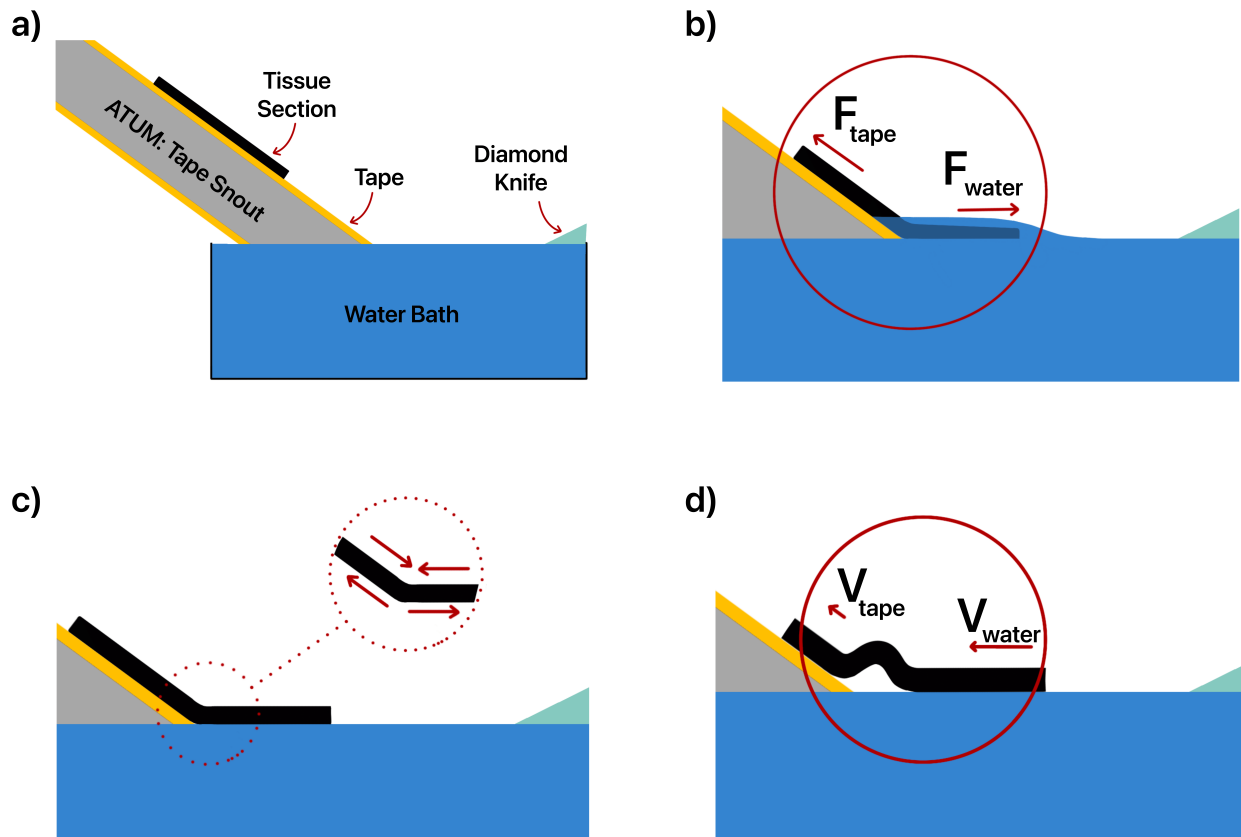


Figure 3.2: Failure Modes of the ATUM Collection System Leading to Tissue Section Damage

These challenges inherent to the automated collection process may explain the higher incidence of sectioning artifacts in projects using ATUM collection compared to manual collection, despite the apparent efficiency advantages of automation.

Although the ATUM collection method adds to this, cracks and folds can occur earlier in the sectioning process, albeit less frequently. The interaction between the knife and sample heterogeneity may create uneven forces during cutting, leading to folds [27]. Furthermore, the MICrONS 1 mm<sup>3</sup> mouse dataset had a pattern of small folds that appear around myelin and blood vessels [36]. This observation is consistent with research showing that increased myelination is correlated with increased stiffness of brain tissue [28]. These local variations in tissue stiffness create conditions favorable for fold formation even before the collection stage.

Improving the collection and cutting procedures will be necessary to remove folds and cracks. However, the ATUM system appears to be the source of the most significant issues and presents greater challenges for mitigation. Since automated collection is essential for scaling connectomics projects, developing an improved collection system should be prioritized while still preserving the benefits necessary for large-scale brain mapping efforts.

### 3.1.2 Partial Sections

Partial sections occur when there is misalignment between the microtome blade and the tissue block. When properly aligned, the knife edge should be parallel to the block face, cutting off complete sections with consistent outlines. However, if misaligned, the knife cuts only through a portion of the tissue, resulting in sections with irregular or truncated shapes. This happens when the cutting plane intersects the block face at an angle rather than being perfectly parallel to it. Complete and consistent section shapes that represent the entire cross-section of the tissue block are essential for successful imaging and reconstruction. Figure 3.3 shows how a change in angle during sectioning can produce partial sections.

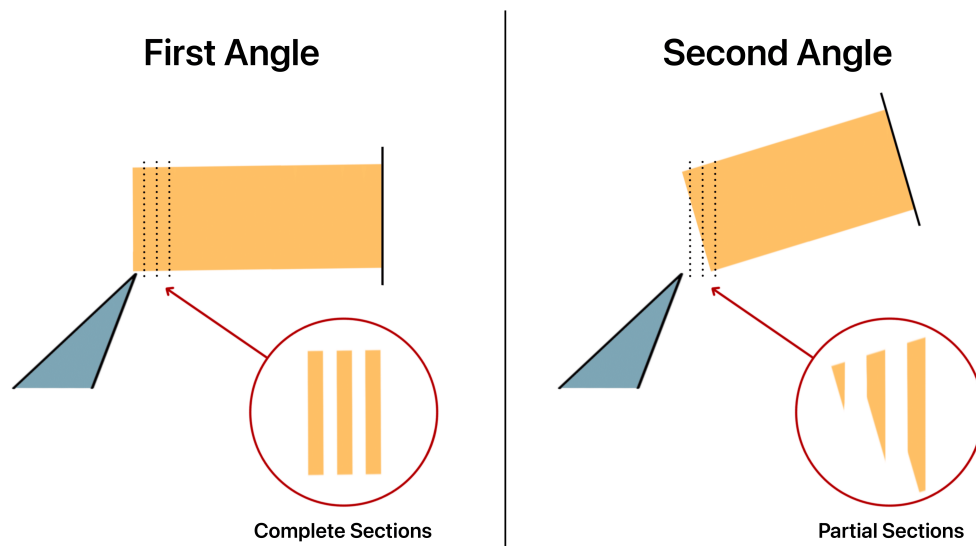


Figure 3.3: Blade Angle Changes Creating Complete versus Partial Sections

During the sectioning of the 1 mm<sup>3</sup> mouse dataset, the blade had to be replaced. Removing and replacing the blade changed its orientation, misaligning it with the block. As a result, 45 sections cut immediately after replacement were partial [16]. The alignment of the images revealed that the misalignment was  $< 0.06^\circ$  [36], a small but sufficient change to cause substantial reconstruction problems. These affected sections required special handling during alignment, as their orientation differed significantly from the remainder of the dataset. Figure 3.4 illustrates the realignment implemented to address this issue. This issue also happened with the human petascale cortical dataset. After knife replacement, the angular misalignment resulted in 30 partial sections with some material loss [39].

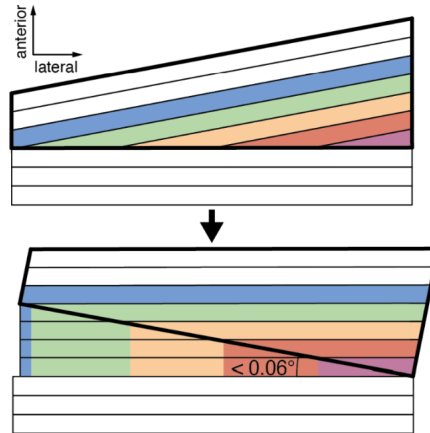


Figure 3.4: Correcting Blade-to-Block Misalignment [36]

The blade fixation method may be unreliable and may introduce variability into the sectioning process due to challenges with consistent blade repositioning. However, there have been no real improvements to the microtome that include sensors or mechanisms that ensure precise blade alignment after replacement, suggesting an urgent need to invest in new hardware solutions.

### 3.1.3 Uneven Thickness

Tissue sections must be cut to a uniform thickness to obtain an accurate scan. Microscopes operate with fixed focal lengths, which causes inaccurate sample representation when section thickness variations push structures too far or too close to the optimal focal plane [40]. This misalignment disrupts the accurate imaging of neural structures, compromising the accuracy of the connectome. Since no system can be built to perfection, it is important to establish acceptable error tolerances. Whether a 1 nm or 10 nm variation is acceptable, quantifying this sets clear performance requirements that the system can be redesigned to meet.

With regard to the underlying causes of thickness variations, thermal expansion during the sectioning process has been identified as a significant factor. As the sample expands thermally, the microtome's pre-set increment no longer determines section thickness; instead, the degree of thermal expansion becomes the controlling factor. Figure 3.5 shows how thermal expansion during cutting can cause a deviation from the expected thickness of the section.

This phenomenon specifically affected data quality in the MICrONS 1 mm<sup>3</sup> mouse visual cortex dataset, where thermal fluctuations compromised sectioning uniformity [16].

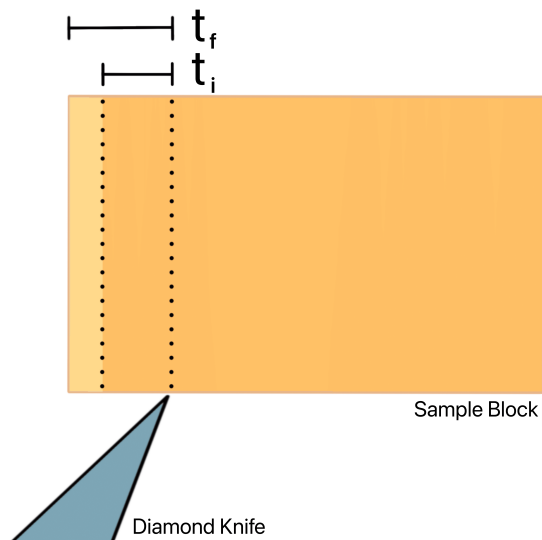


Figure 3.5: Effect of Thermal Expansion on Ultramicrotome Section Thickness

To address this issue, it is important to know how much heat can affect the sectioning process. The thermal behavior of the sample can be calculated using established parameters; the estimates are summarized in Table 3.4.

Parameter	Value
Coefficient of Thermal Expansion ( $\alpha$ )	$9 \times 10^{-6} \text{ } ^\circ\text{C}^{-1}$
Initial Block Length ( $L_0$ )	1 mm
Detectable Dimensional Change ( $\Delta L$ )	5 nm
Estimated Temperature Change ( $\Delta T$ )	$0.55^\circ\text{C}$

Table 3.4: Thermal Expansion Estimates of Epoxy Resin During Sectioning

Due to limited amounts of research on the mechanical properties of the brain, there are no estimates of the thermal expansion properties of brain tissue [28]. Instead, we will estimate the thermal behavior using the properties of the embedding medium, EMS Hard Plus resin. The manufacturer’s datasheet does not provide a thermal expansion coefficient, so for this analysis we can approximate it using a low thermal expansion epoxy coefficient  $9 \times 10^{-6} \text{ } 1/^\circ\text{C}$  [41].

If we consider a sample block with a length of 1 mm that experiences a 5 nm expansion, we can calculate the necessary heat input using the linear thermal expansion formula. We can estimate the thermal expansion using the linear expansion formula:

$$\Delta L = \alpha L_0 \Delta T$$

Rearranged to solve for the temperature change:

$$\Delta T = \frac{\Delta L}{\alpha L_0} = \frac{5 \times 10^{-9} \text{ m}}{(9 \times 10^{-6} \text{ }^\circ\text{C}^{-1})(1 \times 10^{-3} \text{ m})} = 0.55^\circ\text{C}$$

This calculation shows that even a small temperature change of just  $0.55^\circ\text{C}$  would be sufficient to cause a 5 nm expansion in epoxy. This suggests that even minor heat sources, such as warm air currents, could alter the thickness of the section.

The cutting process itself generates heat because of friction in the whole process. Studies have shown that mechanical cutting of meat, a soft tissue, can generate significant heat, raising temperatures by  $11.7^\circ\text{C}$  in beef and  $14.1^\circ\text{C}$  in pork [42]. Although heat generation during the brain sectioning process has not been directly measured, these findings suggest that cutting-generated heat and environmental temperature fluctuations could contribute to the observed expansion.

Beyond thermal effects, microtome setups can also shift, leading to thickness inconsistencies. The process of changing a knife can introduce instability [39]. The position of the knife can change while cutting, sometimes causing it to bump the block and unintentionally damage areas [16]. Microtomes need to be redesigned to improve tool-changing reliability and eliminate existing instability issues.

## 3.2 Material Losses from Sectioning

An understudied phenomenon in connectomics is axial compression, a distortion in which the digitally reconstructed volume ‘shrinks’ along the cutting axis, resulting in dimensions smaller than those of the original physical tissue prior to sectioning. Figure 3.6 illustrates the direction in which this compression manifests itself, specifically along the cutting direction.

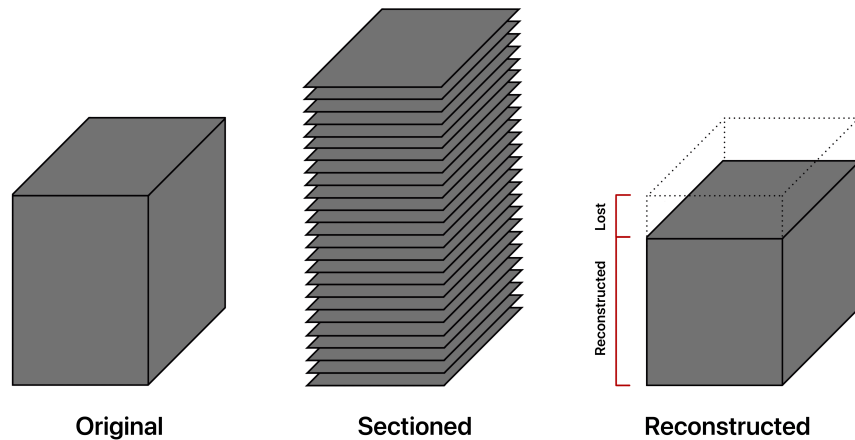


Figure 3.6: Visualization of Compression in Sample Reconstruction

The human  $1 \text{ mm}^3$  temporal cortical connectome dataset shows 28% axial compression, although only three sections were lost out of the entire sample (0.05%) [39]. Since section loss accounts for a negligible portion of this compression, other factors must be responsible. The

compression magnitude matches the estimates in the electron microscopy (EM) sectioning protocols, which consistently document section thickness reductions of 20-30% [43].

The magnitude of this compression warrants further investigation. A reduction in depth could indicate substantial data loss due to distorted or lost structural information within each section. Understanding this phenomenon is crucial for accurate three-dimensional reconstruction and interpretation of the neural tissue architecture. The following are potential mechanisms that cause compression, or in other words, cause material loss.

### 3.2.1 Inevitable Losses

The act of cutting has been shown to destroy material close to the cut edge. This phenomenon is observed in many materials and presumably occurs when cutting brain tissue as well. However, this effect has not yet been quantified in neurological samples. Understanding what parameters control damage is key, as this will help minimize losses. Factors such as cutting speed and cutting angles could all be relevant to minimize damage.

The Lake-Thomas theory, which explains the mechanisms of polymer fracture, has been successfully used to understand how polymer gels fracture [44]. This theory suggests that chemical bonds undergo breakage during the fracture process. Given that hydrogels, a subset of polymer gels, are commonly used as brain tissue phantoms [45], this understanding of molecular damage is particularly relevant for cutting brain tissue. The Lake-Thomas theory has been further developed to account for larger affected regions beyond the molecular plane [46], providing information on broader patterns of soft material. The expanded model identifies the distinct response zones, including a notable damage zone, a finding corroborated by other studies [47]. Figure 3.7 illustrates the spatial distribution of these distinct zones during cutting.

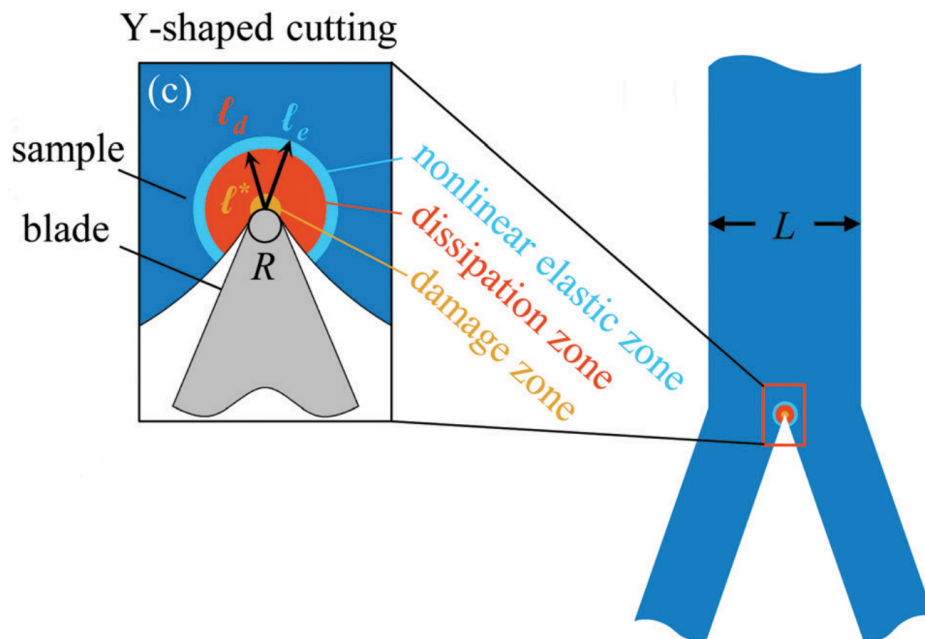


Figure 3.7: Soft Material Fracture Response Zone

In metallic materials, permanent (plastic) deformation occurs within specific stress fields and along slip lines. These phenomena can be measured and predicted to optimize the cutting parameters, ultimately minimizing plastic deformation while maximizing the longevity of the tool and the surface quality [48]. The metal industry pays attention to these effects due to work hardening concerns, a permanent material alteration that accelerates tool wear [49]. Although deformation mechanisms differ between soft tissues and metals, particularly in how the cutting tool engages with the material [47], this parallel underscores the importance of investigating permanent tissue damage during brain cutting procedures.

The significance of this analysis lies in the establishment that cutting brain tissue inherently induces material damage. Understanding the extent of this damage and its contributing factors is crucial to improving current practices. Although more comprehensive research is needed, existing connectome studies have already yielded important insights into this phenomenon.

### 3.2.2 Vibratomes

A critical consideration when using vibratomes is material loss due to kerf, the gap created by the tool's grinding action. Unlike a conventional knife's clean slicing motion, vibratomes operate more like a saw, with the blade moving at high frequencies in the tangential direction, making multiple back-and-forth sawing motions for each forward advancement. This sawing behavior inevitably removes material during cutting, as shown in Figure 3.8.

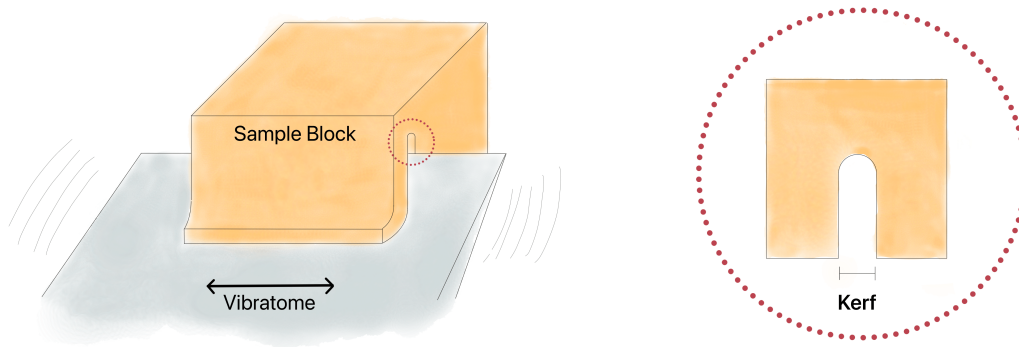


Figure 3.8: Kerf Produced by the Vibratome

The hemibrain connectome of the fruit fly illustrates this loss of material. When using a vibratome to section thick slabs (20 mm) for later processing with FIB-SEM, approximately 30 nm of tissue was lost between consecutive slabs [50]. They used a Diatome diamond knife (Cryo 25°) operating at 39 kHz. Although the knife tip has a diameter of only 4 nm [51], the grinding action resulted in material loss of 30 nm; more than seven times greater than the size of the tool tip. This shows how the sawing motion inherently removes more material than the physical dimensions of the tool would suggest.

Vibratomes are often used because their high-frequency slicing motion reduces cutting forces and tissue deformation during sectioning [43, 52, 53]. However, this benefit comes at

the cost of material loss from the grinding action. Alternative approaches exist that can achieve low-force, low-deformation cutting without as much material loss, as discussed in Chapter 4.

### 3.2.3 Knife Marks

Permanent surface deformations in tissue sections are known as knife marks [37, 43, 52]. Both dulling of the knives and the accumulation of debris are thought to be the cause of them [43, 52]. Knives are frequently cleaned during the sectioning process; specifically, for the MICrONS 1 mm<sup>3</sup> mouse dataset, the knife was cleaned every few hundred sections to maintain section quality [16].

An analogous phenomenon occurs in metal cutting, where "built-up edge marks" appear on the machined surface [54]. In metalworking, these marks develop when broken metal particles adhere to the cutting tool and, due to the heat generated during cutting, weld onto the edge of the tool, as shown in Figure 3.9. This modification of the effective cutting-edge compromises the quality of the surface finish.

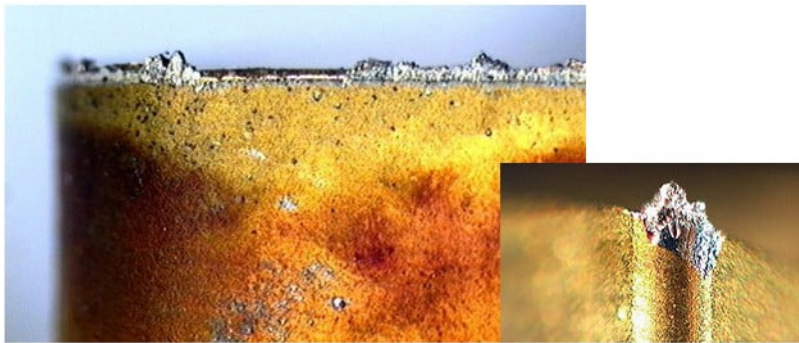


Figure 3.9: Built-Up Edge Formation on Cutting Tool During Metal Cutting [54]

Although tissue sectioning does not involve welding material to the diamond blade, the precise mechanics of how tissue particles accumulate on the blade and subsequently affect surface quality remain poorly understood. The material is lost, but it is not understood where the particles end up. More research is needed to characterize both the particle accumulation process and its relationship to section surface quality.

## 3.3 Tool Wear and Maintenance

Tool wear remains poorly characterized in connectomics, with scientists lacking clear criteria for optimal blade replacement timing. In the MICrONS 1 mm<sup>3</sup> mouse visual cortex dataset, scientists switched the blades three times in the total of 27,972 slices; first after slice 7,930, then after completing 6,843 more slices, and finally using the third blade to complete the remaining 13,199 slices [16]. The 1 mm<sup>3</sup> human temporal cortex dataset demonstrated different switching patterns, with scientists replacing the blade after only 1,695 sections [39].

The cost of blades presents an issue, as three blades for the mouse would cost around a total of \$15,000 using a 4 mm wide 35° or 45° blade, matching the type used for the human

dataset [39, 55] (see Table 3.5). Additionally, blade angling issues occur after reinstallation, leading to partial sections that complicate alignment algorithms, as described in Section 3.1.

Dataset	Blade Switches	Total Sections	Blade Cost (USD)
Mouse Visual Cortex	3	27,972	~15,000
Human Temporal Cortex	1	1,695	~5,000*

\*Estimated based on similar blade type and section count.

Table 3.5: Estimated Costs for Blade Switches for the 1 mm<sup>3</sup> Mouse and Human Connectomes

Drawing parallels to the razor industry, quantification of blade wear remains to minimize costs. Researchers have investigated the mechanisms by which hair damages steel, specifically examining how steel blades dull during hair cutting [56]. Using scanning electron microscopy (SEM) to examine the blades, they discovered that hair creates stress concentrations in the steel that intensify with continued use until portions of the blade eventually chip away. These experiments measured blade wear at 12 nm<sup>3</sup>/nm after five shaving cycles. Similar analytical approaches should be applied to diamond blades used in tissue sectioning. Despite diamond’s exceptional hardness, even nanometer-scale material loss significantly impacts performance, as the blade tip maintains a critical radius of only 2 nm [51].

Given the lack of repeatability when switching blades in the sectioning process and the issues that arise affecting section quality, it is important to minimize wear to maximize the lifetime of a blade. This approach also offers cost improvements. However, more studies are needed to understand which parameters in the cutting process affect blade wear.

# Chapter 4

## Rethinking Sectioning

The quality of the sections that enter the imaging stage is problematic. Both blade-induced defects and collection method flaws create significant obstacles to scaling up for larger volume cutting. Current technologies that are meant to scale, such as the ATUM, produce high error rates. The sectioning process needs a transformation that goes beyond the microtome. This chapter introduces conceptual ideas meant to inspire exploration and guide future design directions.

Error Type	Automation	Improved Collection	Reduced Cutting Force
Cracks	✓	✓	✓
Folds	✓	✓	
Uneven Thickness	✓		✓
Partial Sections	✓		
Material Loss			✓
Knife Wear			✓

Checkmarks indicate solutions that help reduce the corresponding sectioning error.

Table 4.1: Techniques for Mitigating Common Sectioning Errors

### 4.1 Minimizing Forces to Improve Quality

A way to improve the quality of the tissue section surfaces is by reducing the force exerted by the blade onto the tissue. While a theoretical minimum amount of energy is required for cutting, exceeding this threshold redirects excess energy into compressing and damaging the tissue. By decreasing mechanical stress on samples, the section structure is preserved and quality is improved. Minimizing cutting forces not only improves the quality but also extends the lifespan of the diamond blades. Less force means they wear down less over time, resulting in fewer tool changes. This section examines various techniques to minimize the cutting force that should potentially be prototyped.

### 4.1.1 Slicing vs Chopping

Previous studies have established that using a slicing motion significantly reduces the required cutting force in soft tissue sectioning [34, 57]. This technique combines downward pressure with lateral movement, creating more efficient cuts by minimizing tissue deformation. The underlying mechanical principle can be understood through fracture mechanics. The slicing motion combines two fracture modes: Mode I (opening) and Mode III (tearing). Mode III fracture is particularly efficient as it creates separation with minimal bulk deformation of the material. Mode I would be the equivalent of chopping, and is more prone to smashing soft materials.

To help visualize the difference between chopping and slicing, refer to Figure 4.1, showing both cutting methods on a tomato. Applying a pure downward force compresses the tomato (Figure 4.1.1) before the knife ruptures the skin, the tomato is unstable and the initial crack formed is jagged (Figure 4.1.1.c). However, adding a sliding motion (Figure 4.1.2) allows the blade to easily initiate and propagate a clean cut through the skin without smashing the tomato (Figure 4.1.2.b-c). This slicing technique is consistently recommended across culinary instruction [58–60].

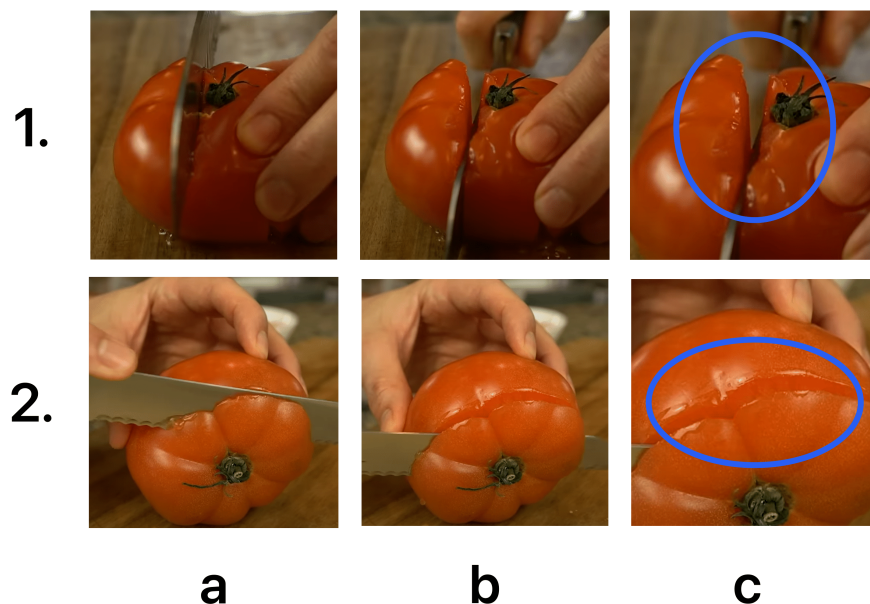


Figure 4.1: Comparing Tomato Cutting Techniques [61]

For connectomics, where sections are cut using diamond knives, this principle becomes particularly important for minimizing tool wear and maintaining consistent section quality. When applying purely vertical force, brain tissue undergoes substantial elastic deformation along the cutting axis, increasing mechanical stress on both the tissue and the cutting edge. The effectiveness of slicing motion is even observable in manual brain sectioning [62, 63].

People instinctively use a slicing motion when cutting brain slabs by hand, even though it is not explicitly recommended in either video [62, 63]. Figure 4.2 breaks the slicing motion

into two orthogonal components:  $F_{\text{push}}$  and  $F_{\text{slice}}$ . These forces act in perpendicular directions, with  $F_{\text{blade}}$  representing the resultant and overall direction of the blade.

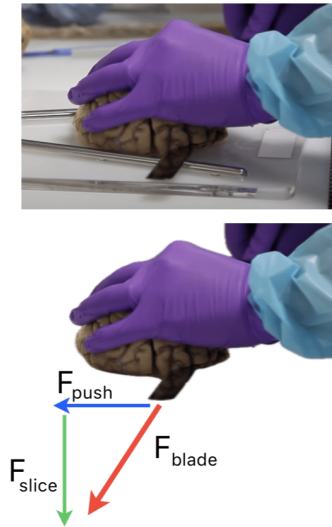


Figure 4.2: Manual Brain Slicing Technique and Force Diagram [62]

Despite the benefits of slicing, only the vibratome offers a cutting method similar to slicing. But as established in Chapter 3, by design it saws away significant amounts of material. Beyond this exception, there are no machines that replicate what humans would instinctively do with their own hands. Figure 4.2 illustrates the brain being supported at multiple contact points: the table with two railings constraining the brain in X and Y, and the hand applying downward pressure for additional stability in Z. This external support system stands in stark contrast to the cantilevered configuration of the sample blocks on a microtome.

### Industrial Applications of Slicing Techniques

Brain tissue sectioning is fundamentally a machining process where the removed material is the desired product. Only a few industries share this focus on valuing what is cut away: foam slicing, veneer sheet production, and food processing industries that specialize in meat, cheese, and vegetable slicing.

These industries deal with viscoelastic materials, just like the brain, so many use slicing in the cutting mechanism. Below are a few examples of the machines used in those industries.

Foam is typically cut with a flexible wire that bends at points of maximum force. This compliance of the wire minimizes deformation of the foam during cutting. Figure 4.3 illustrates a foam slicer in operation. The wire naturally forms an arch-like shape during use, with each side of the arc creating a slice angle that effectively cuts through the material.



Figure 4.3: Wire Slicer for Cutting Foam Sheets [64]

Some kinds of veneer sheet cutting machines utilize a slicing motion. The blade forms an angle with the wood that creates an effective slicing action, as shown in Figure 4.4.

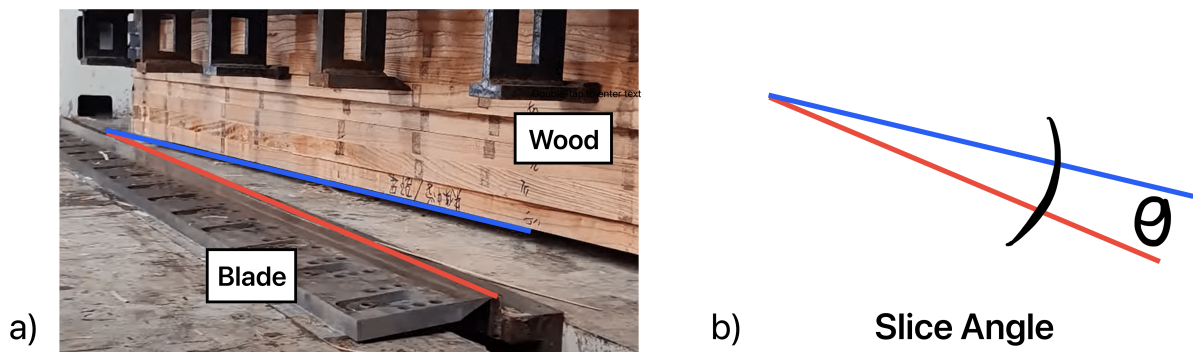


Figure 4.4: Horizontal Wood Veneer Slicer [65]

Industrial cheese and meat slicers employ a rotating blade that descends onto the food at an angle, creating an efficient slicing effect, as illustrated in Figure 4.5.

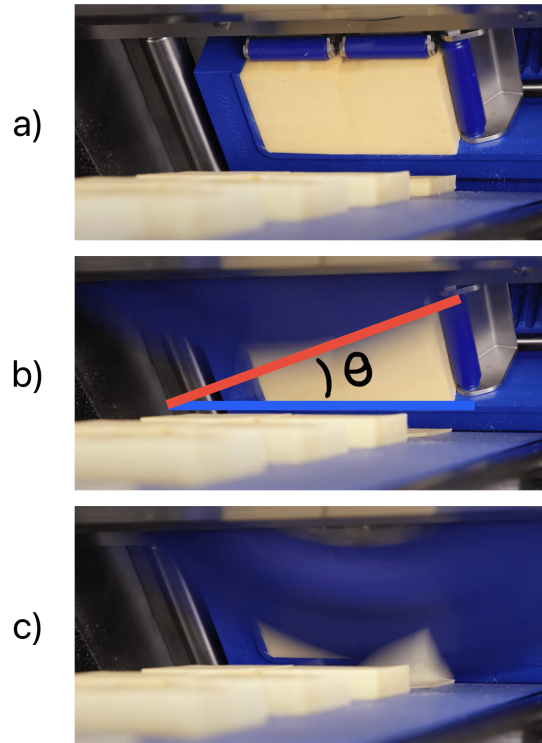


Figure 4.5: Industrial Cheese Slicer [66]

These established technologies for cutting soft materials all implement a slicing motion. The proven effectiveness of slicing in minimizing deformation and facilitating easier cutting should encourage the field of connectomics to move away from the traditional motion of a microtome. While these three industries operate at high volumes, they are not cutting at the nanometer scale. However, the fundamental principles and benefits of slicing remain applicable; it is simply a matter of adapting the technique to this specific application.

### 4.1.2 Embedding Mediums

The embedding medium has a significant impact on the quality and efficiency of the sectioned samples. Current evidence suggests that embedding media properties impact tool wear and cutting success. This is shown in protocols that advise to trim most of the resin to prevent wrinkles and extend the longevity of the diamond knife [67]. The importance of these properties is further exemplified in the preparation of the fruit fly hemibrain connectome, where different resins were strategically used for specific cutting processes; Epon for the initial sectioning process and Durcupan for FIB-SEM to prevent milling streaks [50].

Matching the material properties of the embedding medium with brain tissue could be beneficial. Because these properties are currently different, they respond differently to

cutting forces. This mismatch creates challenges for uniform sectioning due to uneven force distribution that deflects the blade in unpredictable ways.

Figure 4.6 illustrates this phenomenon. When the blade encounters different ratios of embedding medium to tissue along the cutting edge (1a, 2a, 3a), it experiences varying force distributions (1b, 2b, 3b), resulting in different loading conditions on the blade (1c, 2c, 3c).

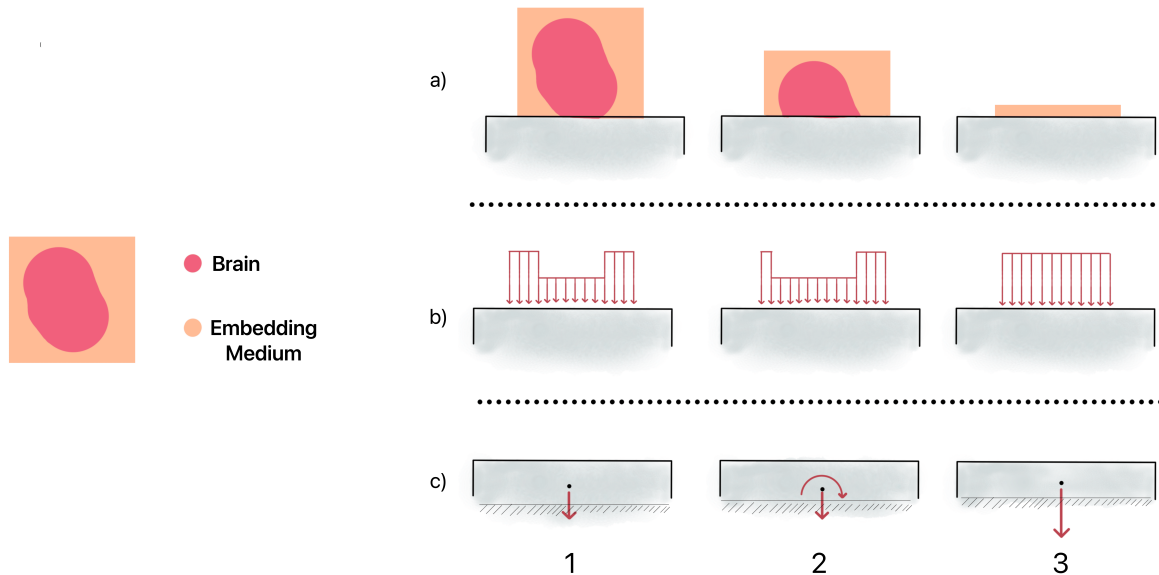


Figure 4.6: Different Loading Scenarios During Progressive Tissue Sectioning

These changing loads cause the blade to wear unevenly, altering the cutting edge over time and potentially introducing inconsistencies in the sectioned tissue surfaces. This mechanical mismatch creates a non-uniform deformation, which causes irregular cuts.

Similar mechanical properties should minimize these deviations in the force distribution, potentially reducing tool wear and improving section quality. However, making the embedding medium as soft as possible has its trade-offs since it minimizes the structural integrity of the entire sample block. The search for the optimal embedding medium is nuanced and represents an important area for further study and optimization.

### 4.1.3 Lubrication to Lower Friction

The fly brain hemibrain connectome project utilized a hot knife technique to section the brain into slabs suitable for FIB-SEM imaging [50, 68]. They used thread cutting oil to reduce an effect called 'stick-slip', where the brain section sticks to the knife during cutting. This approach mirrors common practices in metal machining, where cutting fluids reduce friction between tools and workpieces while dissipating heat [69].

While using thread-cutting oil was an innovative step toward reducing cutting forces, there's room for improvement. The Master Plumber thread cutting oil used has a kinematic viscosity of 27.5-33.5 mm<sup>2</sup>/s at 40°C, qualifying it as an ISO VG 32 oil [70, 71]. Although effective, this viscosity is relatively high. Using a lower-viscosity lubricant could further

reduce friction between the knife and brain section, potentially decreasing the risk of tissue dragging during cutting.

#### 4.1.4 Assisted Cutting

Expanding on the slicing mode, a way to reduce the forces experienced by the blade would be to assist the cut with external means. Using Mode I fracture, the concept involves attaching a mechanism to the slice that helps to remove it while it is being cut, shown in Figure 4.7. This promotes crack propagation and reduces the forces experienced by the blade.

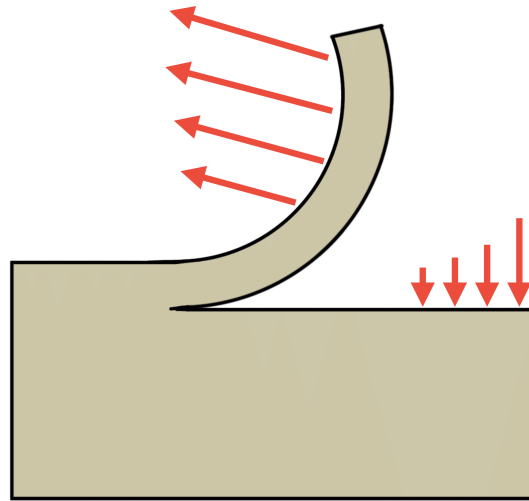


Figure 4.7: Mode I Fracture on Sample Block

This approach offers two key advantages for slice quality. First, the same mechanism that helps peeling can serve as the final support surface during imaging, eliminating the transfer steps where damage could occur. Second, by maintaining continuous control of the slice from cutting through to scanning, we minimize the time the section is 'free-floating' or unsupported, a critical period when distortions or damage often occur. Although coordinating the peeling action with the cutting motion presents engineering challenges, the benefits of continuous slice control could outweigh this complexity.

## 4.2 Improving Section Collection

Sections are currently collected manually or with the ATUM system. Each method has its own trade-offs; manual collection, while generally less prone to error, is labor-intensive and slow. Conversely, ATUM offers significantly higher throughput but frequently results in section artifacts such as cracks and folds, as discussed in Chapter 3. Neither method, in their current forms, is viable for long-term scaling of connectomics.

A major bottleneck in section handling arises from the physical fragility of ultrathin sections. These sections lack structural stability and are particularly susceptible to deformation.

The standard workflow requires the section to traverse from the cutting blade to a water bath prior to collection, a stage during which a high number of errors may be introduced, shown in Figure 4.8.

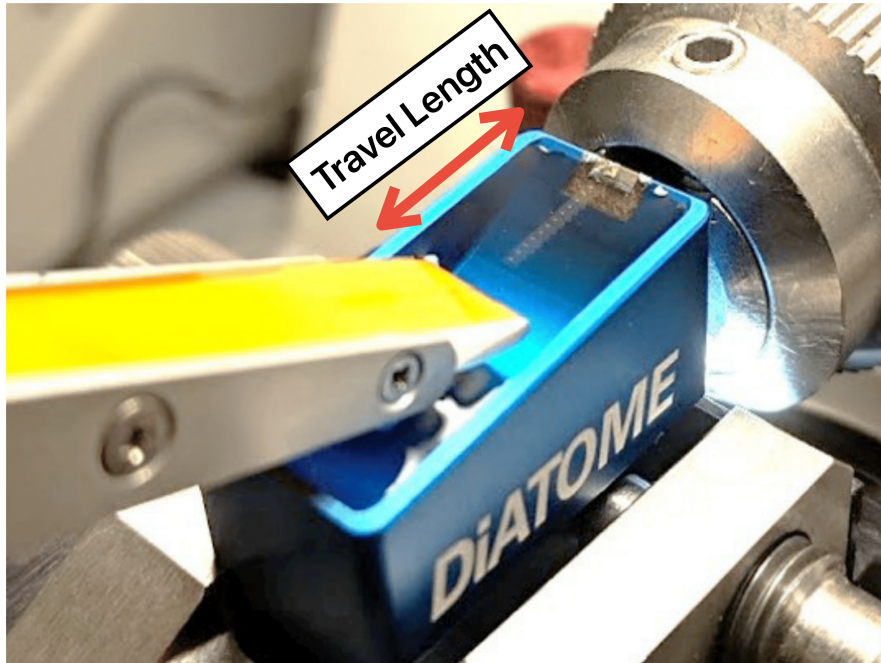


Figure 4.8: Travel Length of Section from Blade to ATUM [72]

Minimizing or altogether eliminating this transitional step could significantly reduce errors. By reducing the time the section spends unsupported and in transit, the section is less likely to sustain damage, as its integrity will not be left to chance. The following are two conceptual approaches that may help address this issue. Although preliminary and speculative, they are intended to spark further design thinking around improved section handling.

#### 4.2.1 Direct Contact

A recently patented approach offers an improvement to the current ATUM system. As shown in Figure 4.9, this new design maintains the core conveyor belt mechanism, but innovates by collecting sections directly from the block face during cutting, potentially reducing deformations [73].

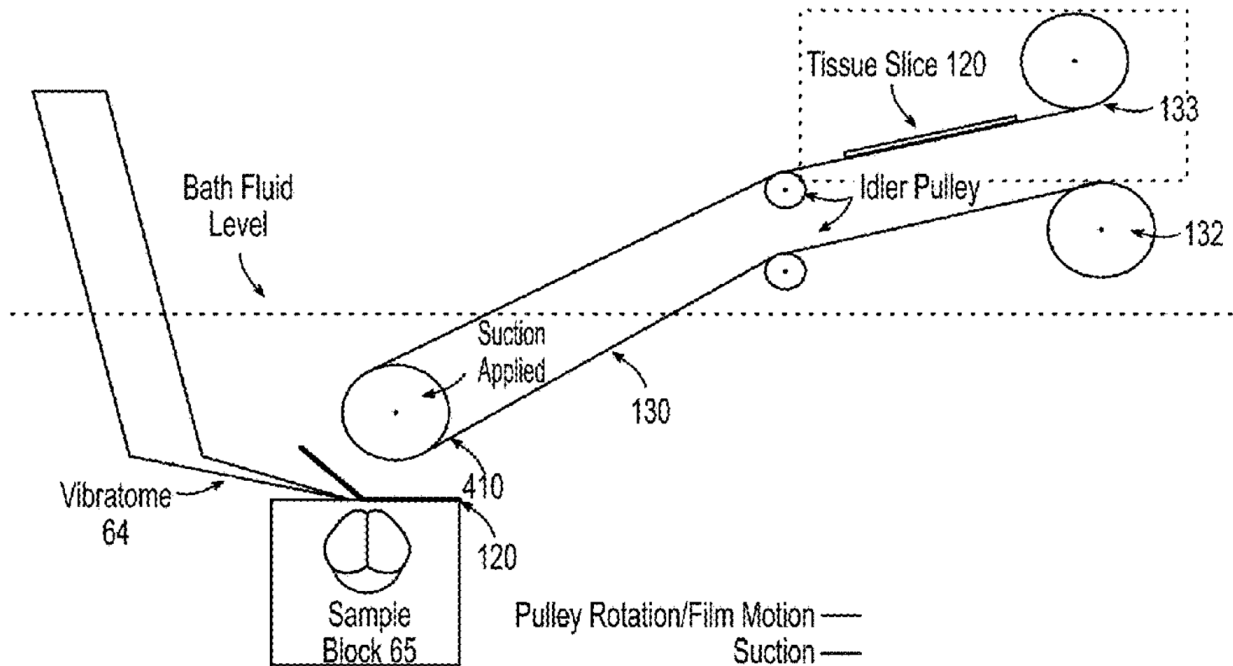


Figure 4.9: Automated Tissue Section Capture System with Conveyor Transport [73]

One of the main benefits of this method is the direct interaction between the freshly cut tissue piece and the conveyor belt. The technique reduces the distance the piece must travel through the fluid by catching it as soon as it is cut. This could potentially lessen the damage, folding, and distortion that occur frequently during this crucial transition.

This method is currently implemented by TissueVision for collecting sections in the 10-1,000 micron range. Its effectiveness for ultrathin sections remains to be validated.

#### 4.2.2 Vertical Collection System

In this concept, after the section is cut and falls into the water bath (Figure 4.10a), a flat collection surface would rise vertically to meet the floating section (Figure 4.10b). The controlled ascent should allow the section to settle onto the platform with minimal disturbance, eliminating the horizontal sliding motion that can introduce folds and cracks. The platform would then retract and move to the section to a storage system. This system could operate at a deliberate pace, as the rate-limiting step in connectomics research remains the imaging process rather than section collection.

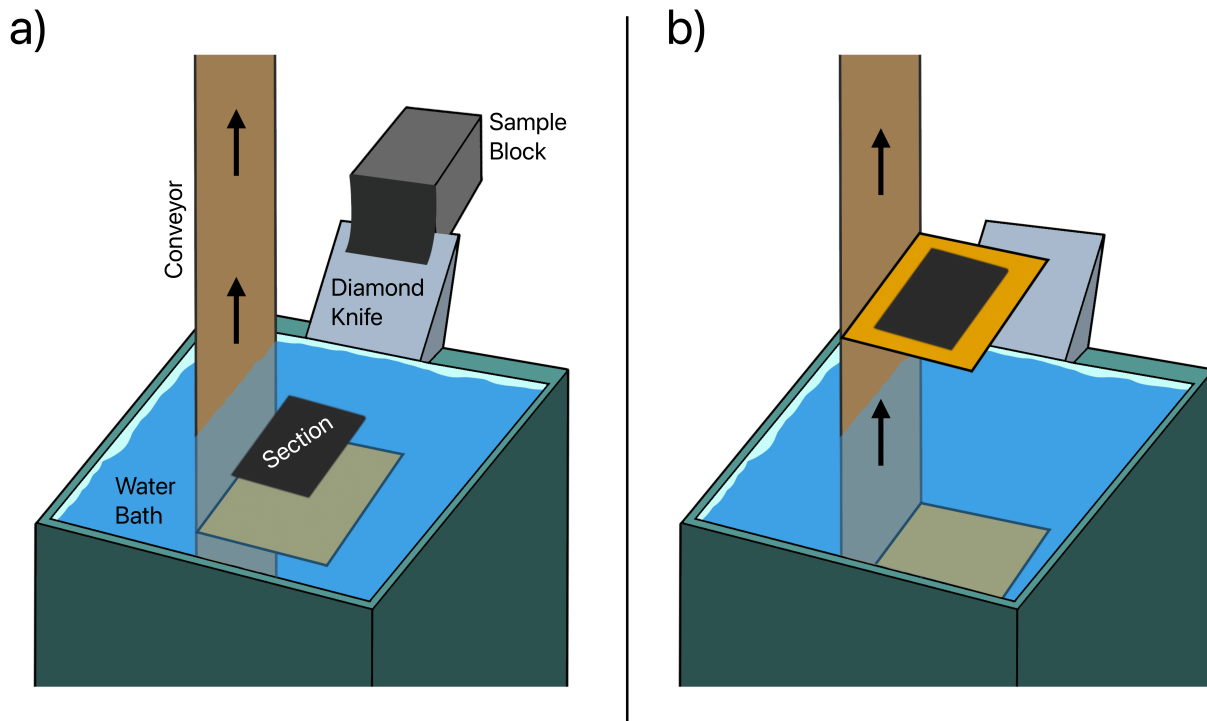


Figure 4.10: Vertical Collection System for Ultrathin Sections

## 4.3 Introducing Automation

The frequency of sectioning errors with current techniques, as detailed in Chapter 3, reveals a lack of adaptability and real-time oversight. Even with the current design of the microtome, without transforming its fundamental cutting mechanism, errors can be prevented with automation. Broadly speaking, automation should achieve these two main functions:

1. **Error Detection:** Monitor and detect sectioning failures in real time and stop operations to prevent more destruction.
2. **Dynamic Adjustment:** Assess cutting conditions and make real-time adjustments based on tissue feedback.

### 4.3.1 Error Detection

At minimum, sectioning and collection equipment should have modes to track and detect failures. With this in place, the process could automatically be stopped when it detects issues such as severe deformation or incomplete cutting, preventing complete specimen destruction. Although more complex monitoring systems could be developed, a simple starting point would be to add cameras connected to the microtome that trigger immediate stops when errors are detected.

### 4.3.2 Dynamic Adjustment

Brain tissue, as discussed in Chapter 2, is viscoelastic and heterogeneous, meaning its behavior and response to cutting varies depending on the region cut and how much time has elapsed. Since the behavior of the tissue varies throughout the cutting process, the parameters of the process should change accordingly. However, current microtomes operate with static parameters (e.g. fixed speed) regardless of any variations.

Unlike machines, human operators naturally modify cutting pressure and speed based on tactile feedback. Although imprecise, this intuitive adjustment allows adaptation to physical variations in material behavior that change with space and time.

Drawing inspiration from this adaptive capability while cutting manually, automated solutions should incorporate systems that detect resistance variations and time-dependent tissue responses, adjusting the cutting parameters accordingly. This dynamic approach would allow for the optimization of the sectioning across heterogeneous tissues while accounting for their viscoelastic and heterogeneous properties, ultimately improving consistency and reducing artifacts and tool wear.



# Chapter 5

## Optimizing Connectomics for Scale

Scaling up connectomics to map increasingly complex neural circuits at the synaptic level requires numerous processes to work at peak performance with high fidelity. However, current connectome creation methods introduce significant errors, primarily during sectioning. These errors stem from design approaches that do not properly account for the numerous interrelated variables that affect quality, cost, and time. Without understanding how these variables interact and create unavoidable trade-offs, researchers rely on intuition rather than quantitative reasoning when making critical process decisions.

Modeling and careful tuning of process variables can help manage trade-offs and improve overall performance. For instance, section thickness presents a critical trade-off. Although thinner sections improve resolution by providing finer data, they are prone to tearing, which can reduce the overall accuracy. Determining the ideal section thickness requires a model that incorporates quantifiable variables with functions that relate them to key performance metrics. This framework allows for parameter optimization to meet specific research goals.

Currently, such models and optimization practices do not exist. This chapter focuses on introducing this method, with special emphasis on the sectioning process. As discussed in Chapter 3, sectioning errors lead to significant data loss and resource-intensive correction efforts, making it important to analyze first. However, the general modeling and optimization framework could be extended to other steps in the connectome creation process.

### 5.1 Defining Success Metrics

Before diving into the optimization model, we must define success criteria. In connectomics, three fundamental metrics provide a consistent basis for evaluating both practical implementation and scientific significance.

- **Quality** refers to the fidelity of data and reconstruction in capturing neural circuitry and synaptic connections. While the definition can vary with research goals, it generally reflects how accurately the connectome represents the original brain tissue.
- **Cost** encompasses the resources required to produce a connectome, including labor, instrumentation, computing infrastructure, and funding. Cost is a critical consideration

for research organizations, funding agencies such as IARPA and NIH [74], and stakeholders in the private sector such as Google, Intel, and Amazon [16] when evaluating scalability and potential returns on investment.

- **Time** refers to the duration required to complete a connectome, from specimen preparation to final reconstruction. To maximize scientific and practical impact, connectome mapping must be achievable in a meaningful timeframe.

These three metrics, quality, cost, and time, form what is commonly referred to as the 'iron triangle' in project management [75], illustrated in Figure 5.1. The concept highlights the inherent trade-offs, where improving one objective often comes at the expense of another. Due to these inevitable compromises, researchers and stakeholders must carefully analyze all available options to make informed decisions that balance research objectives with resource constraints.



Figure 5.1: The Iron Triangle: Good, Fast, or Cheap [76]

Quality, cost, and time function as guiding principles throughout this chapter. In the following sections, we break down the modeling framework, apply it to the sectioning process, and identify specific variables that influence each metric at each step.

## 5.2 Optimization Model Breakdown

The main goal of the modeling framework is to map out how adjustable process variables impact quality, cost, and time, then find the optimal settings that deliver the best possible results.

The heart of the model is the brain state and how it transforms throughout the connectome creation process. Each step subjects the brain to a transformation while also adding to the time and cost. The state of the brain is ultimately what defines the quality of the connectome. For example, a torn brain section will result in a lower quality connectome than an intact one, so steps that might cause tears should be optimized to prevent such damage. The amount of error of the sample entering the imaging stage effectively sets an upper limit on the expected quality of the final connectome. Understanding the condition of the brain before the completed product is crucial for predicting and optimizing the final quality of the connectome.

Figure 5.2 illustrates this model. Each brain state represents the condition of the brain at a given moment, encompassing various properties that change as the tissue progresses through the pipeline. Each action is characterized by parameters (like blade speed for sectioning) and outputs an updated brain state while adding to cumulative cost and time. After all actions are applied, the final brain state determines the resulting quality.

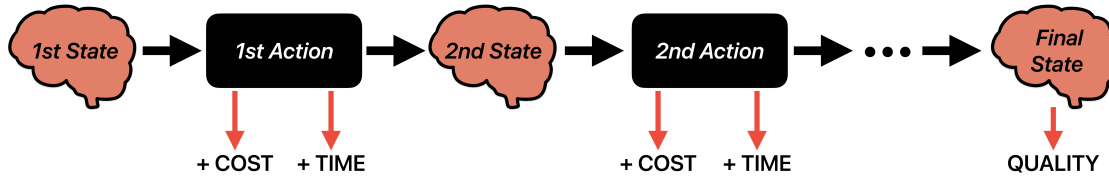


Figure 5.2: Overview of Optimization Model

It’s important to note that some brain characteristics change through these transitions—such as shape, size, or physical integrity—while others remain constant, like species or anatomical region. Both static and dynamic characteristics influence how actions interact with the tissue and how it behaves after going through the action.

The next section will discuss ways to model the sectioning process, focusing on optimizing the physical state of the brain before it enters imaging. Future work should address characterizing the digital brain state, which results from the imaging transition that takes a physical input and produces a digital output.

For optimal results, the connectome process may benefit from a holistic modeling approach that considers all stages together. Rather than optimizing each step in isolation, accounting for their interdependencies could offer better control over overall cost, time, and quality.

## 5.3 Quantifying Sectioning Performance

Requirements for sectioning are currently loosely defined in the field. In many cases, parameters for this process are chosen based on prior experience, intuition, or trial and error rather than empirical evidence. However, as connectomics scales, the need for concrete, quantifiable goals becomes increasingly critical. This section proposes a framework for defining target values for sectioning-specific success metrics—quality, cost, and time—so that future modeling and optimization efforts can be grounded in measurable outcomes.

This discussion proposes a set of metrics that should be quantified in practice. Establishing empirically validated target values and tolerance ranges for each parameter will require future work, tailored to the specific goals and constraints of the connectome being mapped.

### 5.3.1 Quality

Having established that quality is a critical metric of success for evaluating connectomics, we must now define measurable parameters that objectively assess this somewhat abstract

concept. So how do we quantitatively define the quality of brain tissue after it leaves the sectioning process?

Since we consistently frame quality in terms of error minimization in our field, a natural approach is to quantify the specific errors present in sectioned tissue. Quality in sectioned brain tissue can therefore be quantitatively defined through three primary categories of error measurements:

1. **Structural Integrity:** measures tears, folds, and artifacts introduced during sectioning.
2. **Material Recovery:** measures tissue loss during the cutting process or collection.
3. **Dimensional Consistency:** measures thickness variation across the section.

These measurements can be formalized into target values that reflect the specific aims of each connectome effort. These goals guide our optimization efforts as we adjust the sectioning process to achieve desired quality levels. Real-world processes inevitably contain some degree of error. However, this doesn't mean accepting whatever error occurs.

Instead, we should establish tolerance ranges - acceptable error boundaries that balance quality needs with practical constraints. Within the model, this means optimizing parameters for every action in the sectioning process to minimize errors while staying within those defined limits. There's no justification for expending additional resources pursuing perfection when we make room for error.

### 5.3.2 Cumulative Factors: Cost and Time

Quantifying cost and time in the sectioning process follows a straightforward relationship. Each action has identifiable expenses and durations that, when properly tracked, create a clear foundation for minimizing resource expenditure. Although the relationship between actions and their costs is simple, careful documentation becomes crucial as these effects compound at scale.

Table 5.1 outlines the main cost and time variables relevant to the sectioning process.

Table 5.1: Cost and Time Variables in the Sectioning Process

Cost Variables	Time Variables
Diamond blade replacement	Cutting duration
Equipment depreciation	Reset and calibration time
Machine operating costs	Sample collection duration
Labor (manual collection)	Downtime due to malfunctions
Maintenance and repairs	Setup time between samples
Consumables (e.g., lubricants)	Throughput rate

When setting target values for the cost and time of the sectioning process, it's best to focus on order-of-magnitude estimations rather than precise measurements. The difference between projects requiring months versus years is more significant than needing to calculate down to the millisecond.

## 5.4 Sectioning Process Dependencies

Figure 5.3 outlines the relationships between key variables in the sectioning process and the three performance metrics. The brain volume and slice thickness determine how many slices are needed, which sets the total blade travel, essentially, how much work the blade must do. The knife material, blade travel, and cutting speed together influence tool wear. In turn, travel distance and speed define the overall time required for sectioning. Tool wear affects cost, particularly due to blade replacement and maintenance. Most importantly, tool wear also impacts section quality by influencing effective slice thickness and the amount of section loss. These outcomes can be measured to evaluate the quality of the final data.

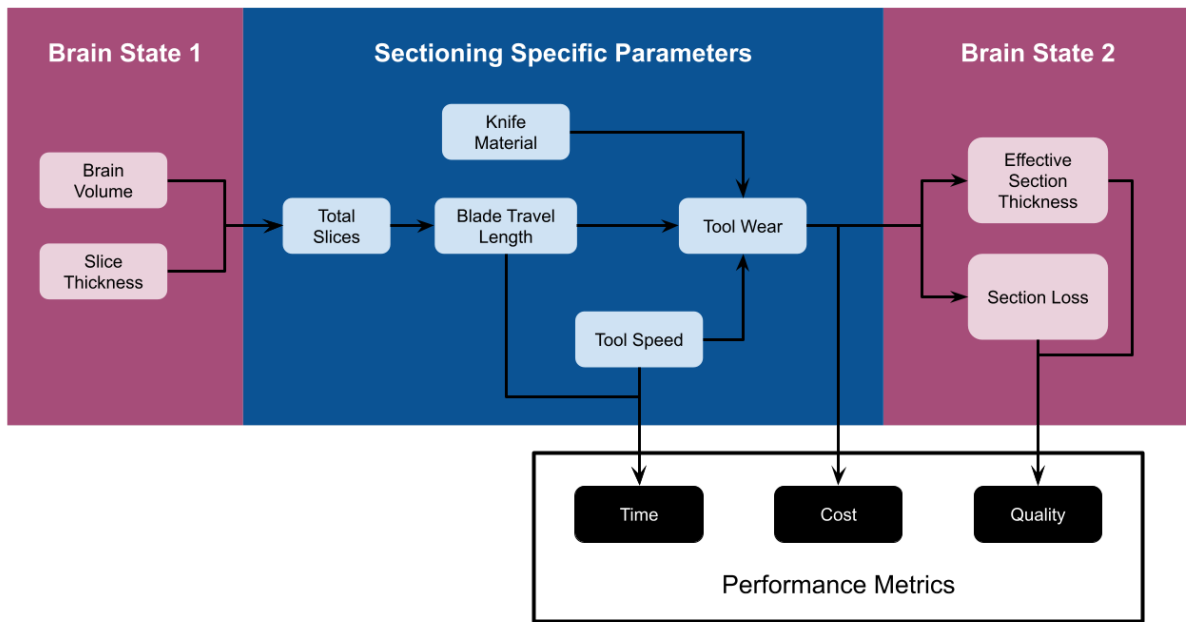


Figure 5.3: Map of Dependencies Relating Diamond Blade Wear

The following simplified scenarios show how some upstream choices could influence tool wear. They are not outcomes shown in the dependency map itself, but rather possible interpretations of the relationships it outlines.

- Increasing section thickness  $\rightarrow$  fewer total slices  $\rightarrow$  less blade travel  $\rightarrow$  reduced wear
- Reducing cutting speed  $\rightarrow$  less tool stress  $\rightarrow$  reduced wear
- Matching embedding stiffness to tissue properties  $\rightarrow$  stable cutting  $\rightarrow$  uniform wear

Tool wear is just one of many interacting factors in the sectioning process, and this representation should be expanded to capture the broader system. Although not yet quantitative, it outlines relationships that future experimental and simulation work can build on to better understand and optimize sectioning performance.



# Chapter 6

## Conclusion

This thesis identifies sectioning as a bottleneck in connectomics. It compiles and analyzes sectioning failures, identifies their physical causes, and approaches them as solvable engineering problems rather than inevitable limitations.

These contributions aim to transform sectioning into a reliable process, laying the groundwork for faster, higher-quality, more scalable, connectome production.

### 6.1 Key Contributions

#### **Identified sectioning as a bottleneck in scaling connectomics**

By analyzing sectioning errors in existing connectomes, this thesis identifies the specific mechanisms behind tissue defects, material losses, and tool wear. These failures incur substantial costs. The ATUM system, over-optimized for speed, introduced cracks and folds, resulting in 28.6% of discarded sections and 25.1% of excluded images in the MICrONS 1 mm<sup>3</sup> dataset, ultimately wasting 1.5 months of imaging time. Left unaddressed, these failure modes will become increasingly costly as connectomics scales to larger volumes.

#### **Reframed sectioning as a solvable engineering problem**

This work shows that sectioning errors are not random or inevitable consequences of working with brain tissue. Through rigorous quantitative analysis, we can identify patterns in sectioning failures, isolate critical variables required for modeling and prediction, and systematically improve results.

#### **Proposed design and optimization strategies for scalable sectioning**

This work identifies three key strategies for advancing sectioning: minimizing cutting forces, improving collection reliability, and implementing intelligent automation. It also presents a practical framework to help see how specific process adjustments affect quality, speed, and cost; replacing intuition-based decisions with measurable, quantitative approaches.

## 6.2 Future Work

Tissue sectioning remains one of the least understood and least optimized steps in the connectomics pipeline, despite its critical importance. This thesis lays the foundation for the transformation of sectioning into a predictable, high-performance process. The following areas represent the most urgent and impactful directions for future work.

### **Tissue Characterization and Predictive Modeling**

Accurate mechanical models are needed to predict the sectioning outcomes under varying conditions. This requires experimental characterization of brain tissue properties like fracture energy and ultimate yield strength. These data are essential to simulate and understand how tissue responds throughout all steps of the sectioning process. Such predictive capabilities would enable the design of optimized sectioning protocols and tooling that reduce error and improve connectome quality.

### **Tool and System Redesign**

The limitations of current microtome designs constrain both section quality and scalability. A clean-slate redesign of the sectioning and collection process is warranted—one that integrates automation, real-time sensing, and innovative cutting mechanics such as guided peeling, compliant wire slicing, and rotary sectioning. These alternative approaches should be evaluated based on their ability to reduce cutting forces, minimize defects, and enable reliable, high-throughput operation. Prioritizing automation and defect resilience from the ground up will be essential for scaling to larger, more complex datasets.

### **Optimizing Process Parameters**

Once sectioning is sufficiently understood, we can create mathematical models that link key process variables (e.g. cutting speed, section thickness) to the relevant outcomes: quality, cost, and throughput. Then, standard optimization methods can be applied to the resulting formula in order to determine optimal parameters, ultimately saving resources and increasing the quality of the final connectome. Developing these models represents a critical area for future research. Such models should initially only take into account sectioning for simplicity, but should eventually include the entirety of the physical process—from sample preparation to reconstruction and analysis—in order to maximize efficiency.

# References

- [1] C. Caruso. *A New Field of Neuroscience Aims to Map Connections in the Brain*. Harvard Medical School, Jan. 2023. URL: <https://hms.harvard.edu/news/new-field-neuroscience-aims-map-connections-brain>.
- [2] S. N. Sotiropoulos and A. Zalesky. “Building connectomes using diffusion MRI: why, how and but”. In: *NMR in Biomedicine* 32.4 (June 2017), e3752. DOI: [10.1002/nbm.3752](https://doi.org/10.1002/nbm.3752).
- [3] L. Silvestri, L. Sacconi, and F. S. Pavone. “The connectomics challenge”. In: *Functional Neurology* 28.3 (July 2013), pp. 167–173. DOI: [10.11138/FNeur/2013.28.3.167](https://doi.org/10.11138/FNeur/2013.28.3.167).
- [4] N. Ohno, M. Katoh, Y. Saitoh, and S. Saitoh. “Recent advancement in the challenges to connectomics”. In: *Microscopy* 65.2 (Dec. 2015), pp. 97–107. DOI: [10.1093/jmicro/dfv371](https://doi.org/10.1093/jmicro/dfv371).
- [5] S. Seung. *I Am My Connectome*. TED, 2010. URL: [https://www.ted.com/talks/sebastian\\_seung\\_i\\_am\\_my\\_connectome](https://www.ted.com/talks/sebastian_seung_i_am_my_connectome) (visited on 04/07/2025).
- [6] E. Gray. “Electron Microscopy of Synaptic Contacts on Dendrite Spines of the Cerebral Cortex”. In: *Nature* 183 (1959), pp. 1592–1593. DOI: [10.1038/1831592a0](https://doi.org/10.1038/1831592a0).
- [7] J. G. White, E. Southgate, J. N. Thomson, and S. Brenner. “The structure of the nervous system of the nematode *Caenorhabditis elegans*”. In: *Philosophical Transactions of the Royal Society of London. Series B, Biological Sciences* 314.1165 (1986), pp. 1–340. DOI: [10.1098/rstb.1986.0056](https://doi.org/10.1098/rstb.1986.0056).
- [8] S. J. Cook et al. “Whole-animal connectomes of both *Caenorhabditis elegans* sexes”. In: *Nature* 571 (2019), pp. 63–71. DOI: [10.1038/s41586-019-1352-7](https://doi.org/10.1038/s41586-019-1352-7).
- [9] P. Schlegel, Y. Yin, A. S. Bates, S. Dorkenwald, K. Eichler, P. Brooks, D. S. Han, M. Gkantia, M. dos Santos, E. J. Munnely, et al. “Whole-brain annotation and multi-connectome cell typing of *Drosophila*”. In: *Nature* 634 (2024), pp. 139–152. DOI: [10.1038/s41586-024-07686-5](https://doi.org/10.1038/s41586-024-07686-5).
- [10] T. Ohyama et al. “A multilevel multimodal circuit enhances action selection in *Drosophila*”. In: *Nature* 520 (2015), pp. 633–639. DOI: [10.1038/nature14297](https://doi.org/10.1038/nature14297).
- [11] R. Shahidi, E. A. Williams, M. Conzelmann, A. Asadulina, C. Verasztó, S. Jasek, L. A. Bezares-Calderón, and G. Jékely. “A serial multiplex immunogold labeling method for identifying peptidergic neurons in connectomes”. In: *eLife* 4 (2015), e11147. DOI: [10.7554/eLife.11147](https://doi.org/10.7554/eLife.11147).
- [12] M. Winding et al. “The connectome of an insect brain”. In: *Science* 379 (2023), eadd9330. DOI: [10.1126/science.add9330](https://doi.org/10.1126/science.add9330).

- [13] Z. Zheng et al. “A Complete Electron Microscopy Volume of the Brain of Adult *Drosophila melanogaster*”. In: *Cell* 174.3 (2018), 730–743.e22. DOI: [10.1016/j.cell.2018.06.022](https://doi.org/10.1016/j.cell.2018.06.022).
- [14] C. Verasztó, S. Jasek, M. Gühmann, L. A. Bezares-Calderón, E. A. Williams, R. Shahidi, and G. Jékely. “Whole-body connectome of a segmented annelid larva”. In: *eLife* 13 (2024), RP97964. DOI: [10.7554/eLife.97964.2](https://doi.org/10.7554/eLife.97964.2).
- [15] A. Shapson-Coe et al. “A petavoxel fragment of human cerebral cortex reconstructed at nanoscale resolution”. In: *Science* 384 (2024), eadk4858. DOI: [10.1126/science.adk4858](https://doi.org/10.1126/science.adk4858).
- [16] The MICrONS Consortium. “Functional connectomics spanning multiple areas of mouse visual cortex”. In: *Nature* 640 (2025), pp. 435–447. DOI: [10.1038/s41586-025-08790-w](https://doi.org/10.1038/s41586-025-08790-w).
- [17] MRC Laboratory of Molecular Biology. *Complete synaptic-resolution connectome of an insect larval brain*. 2023. URL: <https://www2.mrc-lmb.cam.ac.uk/complete-synaptic-resolution-connectome-of-an-insect-larval-brain/> (visited on 04/13/2025).
- [18] MRC Laboratory of Molecular Biology. *Whole brain connectome of fruit fly is most complex brain ever mapped*. MRC Laboratory of Molecular Biology, 2024. URL: <https://www2.mrc-lmb.cam.ac.uk/whole-brain-connectome-of-fruit-fly-is-most-complex-brain-ever-mapped/> (visited on 04/08/2025).
- [19] MICrONS Consortium. *A functional connectome containing 200,000 cells, 75,000 neurons with physiology, and 523 million synapses*. 2021. URL: <https://www.microns-explorer.org/cortical-mm3> (visited on 04/13/2025).
- [20] Google Research. *Ten years of neuroscience at Google yields maps of human brain*. 2024. URL: <https://research.google/blog/ten-years-of-neuroscience-at-google-yields-maps-of-human-brain/> (visited on 04/13/2025).
- [21] C. Grienberger, A. Giovannucci, W. Zeiger, and C. Portera-Cailliau. “Two-photon calcium imaging of neuronal activity”. In: *Nature Reviews Methods Primers* 2 (2022), p. 67. DOI: [10.1038/s43586-022-00147-1](https://doi.org/10.1038/s43586-022-00147-1).
- [22] G. J. Gage, D. R. Kipke, and W. Shain. “Whole Animal Perfusion Fixation for Rodents”. In: *Journal of Visualized Experiments* 65 (2012), e3564. DOI: [10.3791/3564](https://doi.org/10.3791/3564).
- [23] D. B. MacManus. “Excision of whole intact mouse brain”. In: *MethodsX* 10 (2023), p. 102246. ISSN: 2215-0161. DOI: [10.1016/j.mex.2023.102246](https://doi.org/10.1016/j.mex.2023.102246).
- [24] H. H. M. I. (HHMI). *Drosophila Adult Brain Dissection*. YouTube. 2019. URL: <https://www.youtube.com/watch?v=dc9tFpXv0m0> (visited on 04/20/2025).
- [25] Georgia Electron Microscopy. *RMC Ultramicrotomes - Instruments - Gem*. University of Georgia, 2025. URL: <https://gem.uga.edu/instruments/rmc-ultramicrotomes/> (visited on 03/28/2025).
- [26] T. J. Lee et al. “Large-scale neuroanatomy using LASSO: Loop-based Automated Serial Sectioning Operation”. In: *PLOS ONE* 13.10 (2018), e0206172. DOI: [10.1371/journal.pone.0206172](https://doi.org/10.1371/journal.pone.0206172).

- [27] K. J. Hayworth, J. L. Morgan, R. Schalek, D. R. Berger, D. G. C. Hildebrand, and J. W. Lichtman. “Imaging ATUM ultrathin section libraries with WaferMapper: a multi-scale approach to EM reconstruction of neural circuits”. In: *Frontiers in Neural Circuits* 8 (2014). DOI: [10.3389/fncir.2014.00068](https://doi.org/10.3389/fncir.2014.00068).
- [28] S. Budday, T. C. Ovaert, G. A. Holzapfel, P. Steinmann, and E. Kuhl. “Fifty Shades of Brain: A Review on the Mechanical Testing and Modeling of Brain Tissue”. In: *Archives of Computational Methods in Engineering* 27.4 (2020), pp. 1187–1230. DOI: [10.1007/s11831-019-09352-w](https://doi.org/10.1007/s11831-019-09352-w).
- [29] V. P. Astakhov. “Cutting Force Modeling: Genesis, State of the Art, and Development”. In: *Mechanical and Industrial Engineering*. Ed. by J. P. Davim. Materials Forming, Machining and Tribology. Cham: Springer, 2022. DOI: [10.1007/978-3-030-90487-6\\_2](https://doi.org/10.1007/978-3-030-90487-6_2).
- [30] A. T. Zehnder. “Modes of Fracture”. In: *Encyclopedia of Tribology*. Ed. by Q. J. Wang and Y.-W. Chung. Boston, MA: Springer, 2013. DOI: [10.1007/978-0-387-92897-5\\_258](https://doi.org/10.1007/978-0-387-92897-5_258).
- [31] Z. Liu, C. Wang, Z. Chen, and J. Sui. “The advance of surgical blades in cutting soft biological tissue: a review”. In: *International Journal of Advanced Manufacturing Technology* 113 (2021), pp. 1817–1832. DOI: [10.1007/s00170-021-06615-4](https://doi.org/10.1007/s00170-021-06615-4).
- [32] Z. Liu, Z. Liao, D. Wang, C. Wang, C. Song, H. Li, and Y. Liu. “Recent Advances in Soft Biological Tissue Manipulating Technologies”. In: *Chinese Journal of Mechanical Engineering* 35 (2022), p. 89. DOI: [10.1186/s10033-022-00767-4](https://doi.org/10.1186/s10033-022-00767-4).
- [33] J. G. Williams and Y. Patel. “Fundamentals of cutting”. In: *Interface Focus* 6 (2016), p. 20150108. DOI: [10.1098/rsfs.2015.0108](https://doi.org/10.1098/rsfs.2015.0108).
- [34] A. G. Atkins, X. Xu, and G. Jeronimidis. “Cutting, by ‘pressing and slicing,’ of thin floppy slices of materials illustrated by experiments on cheddar cheese and salami”. In: *Journal of Materials Science* 39 (2004), pp. 2761–2766. DOI: [10.1023/B:JMSC.0000021451.17182.86](https://doi.org/10.1023/B:JMSC.0000021451.17182.86).
- [35] C. E. Dougan, Z. Song, H. Fu, A. J. Crosby, S. Cai, and S. R. Peyton. “Cavitation induced fracture of intact brain tissue”. In: *Biophysical Journal* 121.14 (2022), pp. 2721–2729. DOI: [10.1016/j.bpj.2022.06.016](https://doi.org/10.1016/j.bpj.2022.06.016).
- [36] T. Macrina et al. “Petascale neural circuit reconstruction: automated methods”. In: *bioRxiv* (2021). Preprint. DOI: [10.1101/2021.08.04.455162](https://doi.org/10.1101/2021.08.04.455162).
- [37] J. S. Phelps et al. “Reconstruction of motor control circuits in adult *Drosophila* using automated transmission electron microscopy”. In: *Cell* 184.3 (2021), 759–774.e18. DOI: [10.1016/j.cell.2020.12.013](https://doi.org/10.1016/j.cell.2020.12.013).
- [38] Luxel Corporation. *TEM Sample Supports*. Luxel Corporation Website. 2024. URL: <https://luxel.com/products/tem-supports/> (visited on 04/15/2025).
- [39] A. Shapson-Coe et al. “A connectomic study of a petascale fragment of human cerebral cortex”. In: *bioRxiv* (2021). Preprint. DOI: [10.1101/2021.05.29.446289](https://doi.org/10.1101/2021.05.29.446289).
- [40] J. Brownrout and R. Kirmse. *High Quality Sectioning in Ultramicrotomy*. Leica Microsystems, 2023. URL: <https://www.leica-microsystems.com/science-lab/life-science/high-quality-sectioning-in-ultramicrotomy/> (visited on 04/15/2025).

- [41] Master Bond Inc. *Epoxies with Low Coefficient of Thermal Expansion*. 2025. URL: <https://www.masterbond.com/properties/epoxies-low-coefficient-thermal-expansion> (visited on 01/20/2025).
- [42] D. Ianitchi, V. Bacita, G. V. Bahaciu, L. Nistor, L. Urdes, and C. Hodosan. “Changes in Temperature, the Heat Released and the Power Required for Chopping Meat”. In: *Scientific Papers: Animal Science and Biotechnologies* 43.2 (2010). Available from CABI Digital Library. URL: <https://www.cabidigitallibrary.org/doi/pdf/10.5555/20123107645>.
- [43] I. Moradi and M. Behjati. “Six common errors cause dangerous mistakes in interpretation of electron micrographs”. In: *Microscopy Research and Technique* 75.5 (May 2012), pp. 677–682. DOI: [10.1002/jemt.21111](https://doi.org/10.1002/jemt.21111).
- [44] T. Sakai, Y. Akagi, S. Kondo, and U. Chung. “Experimental verification of fracture mechanism for polymer gels with controlled network structure”. In: *Soft Matter* 10 (35 2014), pp. 6658–6665. DOI: [10.1039/C4SM00709C](https://doi.org/10.1039/C4SM00709C).
- [45] A. S. Vanina et al. “A hydrogel-based phantom of the brain tissue aimed at modelling complex metabolic transport processes”. In: *European Physical Journal Special Topics* 232 (2023), pp. 475–483. ISSN: 1951-6355. DOI: [10.1140/epjs/s11734-022-00733-0](https://doi.org/10.1140/epjs/s11734-022-00733-0).
- [46] B. Zhang and S. B. Hutchens. “On the relationship between cutting and tearing in soft elastic solids”. In: *Soft Matter* 17 (28 2021), pp. 6728–6741. DOI: [10.1039/D1SM00527H](https://doi.org/10.1039/D1SM00527H).
- [47] B. Zhang, C. S. Shiang, S. Yang, and S. B. Hutchens. “Y-Shaped Cutting for the Systematic Characterization of Cutting and Tearing”. In: *Experimental Mechanics* 59 (2019), pp. 517–529. ISSN: 0014-4851. DOI: [10.1007/s11340-019-00479-2](https://doi.org/10.1007/s11340-019-00479-2).
- [48] Z. Yang, X. Zhang, G. Nie, D. Zhang, and H. Ding. “A Comprehensive Experiment-Based Approach to Generate Stress Field and Slip Lines in Cutting Process”. In: *Journal of Manufacturing Science and Engineering* 143.7 (July 2021), p. 071014. DOI: [10.1115/1.4049848](https://doi.org/10.1115/1.4049848).
- [49] C. Yue, X. Liu, J. Ma, Z. Jia, and Z. Li. “Hardening effect on machined surface for precise hard cutting process with consideration of tool wear”. In: *Chinese Journal of Mechanical Engineering* 27 (2014), pp. 1249–1256. ISSN: 1000-9345. DOI: [10.3901/CJME.2014.0922.154](https://doi.org/10.3901/CJME.2014.0922.154).
- [50] L. K. Scheffer et al. “A connectome and analysis of the adult *Drosophila* central brain”. In: *eLife* 9 (2020), e57443. DOI: [10.7554/eLife.57443](https://doi.org/10.7554/eLife.57443).
- [51] DiATOME. *Why use DiATOME*. n.d. URL: <https://www.diatomeknives.com/why-use-diatome> (visited on 04/15/2025).
- [52] J. Wang, C. Li, and S.-C. Chen. “Sectioning soft materials with an oscillating blade”. In: *Precision Engineering* 56 (2019), pp. 96–100. ISSN: 0141-6359. DOI: [10.1016/j.precisioneng.2018.11.002](https://doi.org/10.1016/j.precisioneng.2018.11.002).
- [53] D. Studer and H. Gnaegi. “Minimal compression of ultrathin sections with use of an oscillating diamond knife”. In: *Journal of Microscopy* 197.Pt 1 (Jan. 2000), pp. 94–100. DOI: [10.1046/j.1365-2818.2000.00638.x](https://doi.org/10.1046/j.1365-2818.2000.00638.x).

- [54] Harvey Performance Company. *Causes & Effects of Built-Up Edge (BUE) in Turning Applications*. n.d. URL: <https://www.harveyperformance.com/in-the-loupe/causes-effects-of-built-up-edge-bue-in-turning-applications/> (visited on 01/20/2025).
- [55] DiATOME. *DiATOME Diamond Blades & Knives Prices*. DiATOME U.S., 2025. URL: <https://www.diatomeknives.com/prices> (visited on 01/12/2025).
- [56] G. Roscioli, S. M. Taheri-Mousavi, and C. C. Tasan. “How hair deforms steel”. In: *Science* 369 (2020), pp. 689–694. DOI: [10.1126/science.aba9490](https://doi.org/10.1126/science.aba9490).
- [57] E. Reyssat, T. Tallinen, M. Le Merrer, and L. Mahadevan. “Slicing Softly with Shear”. In: *Phys. Rev. Lett.* 109.24 (Dec. 2012), p. 244301. DOI: [10.1103/PhysRevLett.109.244301](https://doi.org/10.1103/PhysRevLett.109.244301).
- [58] Allrecipes. *Basic Knife Skills | Allrecipes*. 2010-06-12. URL: [https://www.youtube.com/watch?v=Ydc\\_SaQ\\_eRQ](https://www.youtube.com/watch?v=Ydc_SaQ_eRQ) (visited on 04/15/2025).
- [59] J. K. López-Alt. *Knife Skills: The 4 Knife Cuts Every Cook Should Know*. 2014. URL: <https://www.serious-eats.com/draftknife-skills-the-three-basic-knife-cuts> (visited on 04/15/2025).
- [60] J. Moskin. *Basic Knife Skills*. Photographs by Karsten Moran. 2025. URL: <https://cooking.nytimes.com/article/basic-knife-skills> (visited on 04/15/2025).
- [61] Mashed. *You’ve Been Cutting Tomatoes Wrong This Whole Time*. YouTube, Apr. 6, 2020. URL: <https://www.youtube.com/watch?v=62uSxjVSxUA> (visited on 04/15/2025).
- [62] W. Collection. *Dissecting Brains*. YouTube, May 10, 2012. URL: <https://www.youtube.com/watch?v=OMqWRlxo1oQ> (visited on 04/15/2025).
- [63] C. Biological. *Carolina Quick Tip®: Sheep Brain Dissection*. YouTube, Jan. 3, 2014. URL: <https://www.youtube.com/watch?v=o3v9cdD6Ssqo> (visited on 04/15/2025).
- [64] Fabric Supply. *Foam Rubber Slicer*. Website. Fabric Supply, Inc., 2025. URL: <https://fabricsupply.com/products/foam-rubber-slicer/> (visited on 04/15/2025).
- [65] C. P. Machine-Lucinda. *How to make Sliced veneer / Planed veneer by Horizontal Veneer slicer / Veneer slicing machine?* YouTube, Apr. 25, 2024. URL: <https://www.youtube.com/watch?v=r-wWgdivGbA> (visited on 04/15/2025).
- [66] W. F. Technology. *Compact slicer with power | Weber weSLICE 1000*. YouTube, Apr. 16, 2024. URL: <https://www.youtube.com/watch?v=2PATbiDrVto> (visited on 04/15/2025).
- [67] V. Baena, R. L. Schalek, J. W. Lichtman, and M. Terasaki. “Serial-section electron microscopy using automated tape-collecting ultramicrotome (ATUM)”. In: *Three-Dimensional Electron Microscopy*. Ed. by T. Müller-Reichert and G. Pigino. Vol. 152. Methods in Cell Biology. Academic Press, 2019, pp. 41–67. DOI: [10.1016/bs.mcb.2019.04.004](https://doi.org/10.1016/bs.mcb.2019.04.004).
- [68] K. J. Hayworth, C. S. Xu, Z. Lu, G. W. Knott, R. D. Fetter, J. C. Tapia, J. W. Lichtman, and H. F. Hess. “Ultrastructurally smooth thick partitioning and volume stitching for large-scale connectomics”. In: *Nature Methods* 12 (2015), pp. 319–322. DOI: [10.1038/nmeth.3292](https://doi.org/10.1038/nmeth.3292).
- [69] Seco Tools. *Lubrication in Metalworking*. Seco Tools, 2025. URL: <https://www.secotools.com/article/126229?language=en> (visited on 01/12/2025).

- [70] William H. Harvey Company. *Harvey Thread Cutting Oil*. Safety Data Sheet 3355E. Version 01. Omaha, NE: William H. Harvey Company, May 2015.
- [71] Anton Paar GmbH. *ISO Viscosity Classification*. Anton Paar GmbH, n.d. URL: <https://wiki.anton-paar.com/en/iso-viscosity-classification/> (visited on 04/15/2025).
- [72] RMC Boeckeler. *Versatility of Automated Tape-collecting Ultramicrotomy (ATUM) with the RMC Boeckeler ATUMtome*. Application Note. RMC Boeckeler, May 2022. URL: [https://boeckeler.com/wp-content/uploads/2022/05/AN\\_ATUM\\_Versatility-of-Automated-Tape-collecting-Ultramicrotomy-ATUM-with-the-RMC-Boeckeler-ATUMtome.pdf](https://boeckeler.com/wp-content/uploads/2022/05/AN_ATUM_Versatility-of-Automated-Tape-collecting-Ultramicrotomy-ATUM-with-the-RMC-Boeckeler-ATUMtome.pdf) (visited on 04/20/2025).
- [73] S. E. Anderson, E. Yew, P. Knodle, and T. Ragan. “Automated tissue section capture, indexing and storage system and methods”. Patent 12135261. I. TissueVision. Nov. 2024.
- [74] M. Eisenstein. “Putting the mouse brain on the map”. In: *Nature* 628 (Apr. 2024), pp. 677–679. DOI: [10.1038/d41586-024-01096-3](https://doi.org/10.1038/d41586-024-01096-3).
- [75] J. Pollack, J. Helm, and D. Adler. “What is the Iron Triangle, and how has it changed?” In: *International Journal of Managing Projects in Business* 11.2 (2018), pp. 527–547. DOI: [10.1108/IJMPB-09-2017-0107](https://doi.org/10.1108/IJMPB-09-2017-0107).
- [76] S. Thurrott. *Good, Fast, or Cheap: Pick 2 to Grow Your Business*. 2021. URL: <https://medium.com/swlh/good-fast-or-cheap-pick-2-to-grow-your-business-7b37bf928a1> (visited on 03/31/2025).